A Quantitative Analysis of the biological pump in the oligotrophic subtropical North Atlantic

Dissertation
zur Erlangung des Doktorgrades
der Christian-Albrechts-Universität
zu Kiel

vorgelegt von
Heiner Dietze

Kiel
2004

Referent	Prof. Dr. Andreas Oschlies
Korreferent	Prof. Dr. Jürgen Willebrand
Tag der mündlichen Prüfung:	3.6.2004
Zum Druck genehmigt:	29.5.2004

Zusammenfassung

Die Ozeane stellen auf Zeitskalen welche kürzer sind als geologische das mit Abstand größte globale Kohlenstoffreservoir. Die Konzentration von Kohlendioxid, einem der relevantesten "Treibhausgase" in der Atmosphäre entspricht nicht einmal 2% des ozeanischen Bestandes. Dies verdeutlicht, dass ein Verständnis globaler Klimaveränderungen mit einem quantitativen Verständnis derjenigen Prozesse einhergehen muss, die den Kohlenstoffgehalt in den Ozeanen steuern. Das Ziel dieser Arbeit ist es zu einem besseren Verständnis eben dieser Mechanismen im Nordatlantik beizusteuern.

Im Mittelpunkt steht der oligotrophe subtropische Wirbel. In dieser Region wird sowohl die Größenordnung als auch die Richtung des Kohlenstoffaustausches zwischen Ozean und Atmosphäre kontrovers diskutiert. Der Grund hierfür sind inkonsistente Abschätzungen von biologisch induziertem Kohlenstoffexport, abgeleitet aus Sauerstoffzehrungsraten in der Thermokline und lokalen Messungen von Nährstofftransport in die oberflächennahe Schicht.

Vorgestellt werden Beobachtungen und Ergebnisse eines biogeochemischen Ozeanmodells, welche zeigen, dass die Diskrepanz zwischen Nährstofftransport in die oberflächennahe Schicht und Sauerstoffzehrung in der Tiefe um 20% reduziert wird, wenn bis dahin vernachlässigte physikalische Prozesse berücksichtigt werden. Die verbleibenden 80% werden Stickstofffixierung und Subduktion von gelöstem organischem Kohlenstoff zugeschrieben.

Darüber hinaus wird ein Vorbehalt gegenüber einer weit verbreiteten Methode zur Trennung zwischen physikalisch und biologisch induziertem Sauerstoffaustausch zwischen Ozean und Atmosphäre geäußert.

Abstract

The oceans are by far the largest global reservoir of carbon that is available on shorter than geological timescales. Its stock exceeds by more than 50 times the atmospheric inventory of carbon dioxide, a key "greenhouse" gas. Thus it is evident that the understanding of global climate change must be accompanied with a quantitative understanding of mechanisms governing the carbon inventory of the oceans. The aim of this thesis is to improve our understanding of these mechanisms in the North Atlantic Ocean.

The focus is on the oligotrophic subtropical gyre, where the magnitude and even the direction of its biotic contribution to the air-sea flux of carbon dioxide is subject to a controversy. This controversy is based on an inconsistency between estimates of biotically-effected carbon export inferred from oxygen utilisation rates in the thermocline and local measurements of turbulent nitrate supply to the surface layer.

Observational data and results from an eddy-permitting biogeochemical ocean model presented here, indicate that the mismatch between nitrate supply to the surface layer and oxygen utilisation at depth is reduced by 20% if physical processes previously neglected are accounted for. The remaining 80% are ascribed to biogeochemical processes, namely nitrogen fixation and subduction of dissolved organic carbon.

In addition a caveat concerning a standard method used to distinguish between physically and biotically effected air-sea oxygen fluxes is reported.

Introduction

"The Earth's climate system has demonstrably changed on both global and regional scales since the pre-industrial era, with some of these changes attributable to human activities" (WATSON AND ALBRITTON (2001)). One of these "human activities" is the anthropogenic emission of so-called "greenhouse gases" into the atmosphere where they absorb a fraction of the outgoing infrared radiation which the Earth emits to space to compensate for the incoming solar short wave irradiation. Increasing the concentration of these gases results in an imbalanced radiation budget of the Earth and subsequent net warming of the Earths surface. This effect of anthropogenic "greenhouse gases" is also referred to as radiative forcing.

Most of the anthropogenic radiative forcing is ascribed to increasing atmospheric CO_2 concentrations. CO_2 content of air bubbles trapped in polar ice caps reveals that around the year 1750 atmospheric levels started to rise at an unprecendented rate after relatively stable conditions throughout the holocene. During 1994 the highest level ever since 220,000 years was reached. Evidence indicating that this rise in atmospheric CO_2 concentration is anthropogenically effected include: (1) an emission history from fossil fuel combustion and land use changes parallel to atmospheric CO_2 levels, (2) an increase of atmospheric CO_2 concentrations in the southern hemisphere lagging behind levels observed in the northern hemisphere where more fossil fuel is combusted and (3) characteristic isotopic signatures of fossil fuel leaving their mark in the atmosphere (SHIMEL ET AL. (2001)).

Based on its positive radiative forcing and its considerable anthropogenic emission it is generally assumed that the atmospheric CO_2 concentration will be a critical factor determining the future of our climate.

The crucial point limiting our ability to forecast atmospheric CO_2 concentrations is that the fate of CO_2 emitted into the atmosphere is not known. Currently, the main "active" global reservoirs of carbon are the oceans while the terrestrial biosphere including soils and the atmosphere contain 5% and 2% of the oceanic carbon stock, respectively. However, it might well be the case that this partition is subject to changes (e.g. in a warming climate). Until now, processes keeping the carbon in the respective stocks are not comprehensively understood. Especially the role of the oceans is still unclear, a fact that was epitomized in hindcasts of atmospheric CO_2 concentrations during the last glacial maximum based on biogeochemical ocean circulation models (ARCHER ET AL. (2000)). Air trapped in glacial ice indicates that atmospheric CO_2 concentrations were reduced by 30%

during that time. Moreover there is evidence that the terrestrial carbon stock was also reduced (e.g. CRAWLEY (1995)), so that the oceanic pool must have been increased relative to present-day conditions. Biogeochemical ocean circulation models still fail to incorporate that surplus of carbon during glacial conditions.
Carbon, here referred to as the sum of dissolved inorganic carbon (DIC), dissolved organic carbon (DOC) and particulate organic carbon (POC) is not homogeneously distributed in the oceans. Most salient is a vertical gradient, with deep water containing more carbon than surface water. As there is at least one process (e.g. vertical turbulent diffusion) homogenizing the ocean there must be an opposing mechanism which continuously transports carbon from the surface layer to the deep ocean (implicitly assuming that the ocean is in steady state). Two processes are distinguished, referred to as the "physical (or solubility) pump" and the "biological pump" of carbon.
The physical pump of carbon is connected to the thermohaline circulation and a consequence of CO_2 being more soluble in colder water. In regions of deep water formation cold surface water with high DIC concentrations is shielded from the surface and subsequently spreads all over the deep oceans.
The "biological pump" of carbon refers to marine phytoplankton assimilating dissolved inorganic carbon into dissolved or particulate organic material within the sun-lit surface ocean. Part of the particulate fraction sinks into the deep ocean. Heteorotrophic organisms feed on it so most of the POC is remineralized on its way down to the sea floor thus increasing the DIC concentration of the deep ocean relative to the surface. Only an evanescent fraction reaches the sea floor and allows for burial of carbon in sediments. DOC is different as it does not sink through the water. Hence it can only contribute to the "biological pump" in regions of net downward velocities (e.g. in the subtropical gyres).
At present it seems that a deficient understanding of the "biological pump" as regards its parameterization in biogeochemical ocean models limits our capability of modeling glacial-interglacial CO_2 variations and consequently reduces confidence in forecasts of such models. The argument is that the solubility pump was probably a minor player reducing glacial atmospheric CO_2 levels, since the large, deep-water reservoirs of carbon could not have cooled and increased their solubility enough to dominate as they are quite close to freezing even today (BROECKER AND PENG (1998), SIGMAN AND BOYLE (2000)).
Another reason to focus on biologically mediated processes is that the "biological pump" is the only remaining oceanic mechanism potentially buffering anthropogenic CO_2 emission in a warming climate since the solubility pump will be reduced in its capacity to sequester carbon dioxide away from the atmosphere as warming of water results in lower solubility.
A rough calculation of the strength of the "biological pump" based on vertical nutrient gradients puts the potential of a modulation into perspective:
Fig. 0.1 shows the global mean vertical gradient of phosphate which corresponds to vertical diffusive carbon fluxes assuming a constant Redfield ratio (C:N:P = 106:16:1) and a mean global vertical diffusivity of $10^{-4}\mathrm{m}^2/\mathrm{s}$. (This diffusivity was calculated by MUNK AND WUNSCH (1998) implicitly assuming

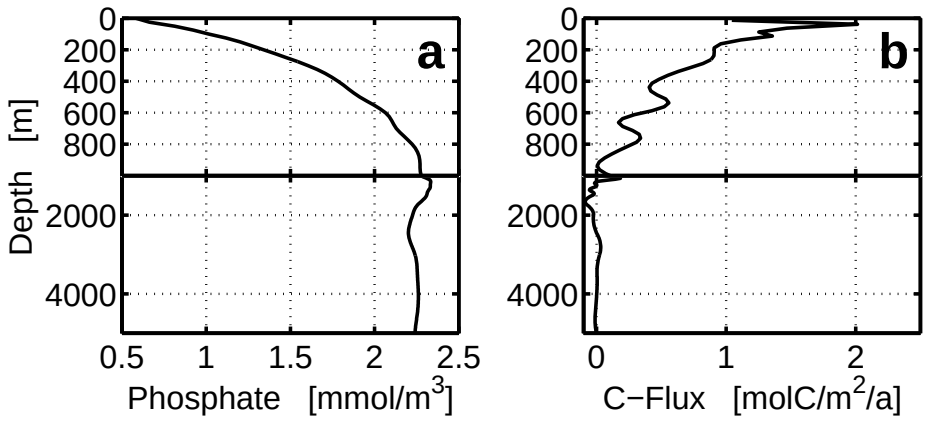

Figure 0.1: (a) global mean vertical profile of PO_4 derived from the climatology of CONKRIGHT ET AL. (1994). (b) global mean of vertical diffusive carbon flux calculated from the global mean vertical profile of PO_4 assuming a global mean vertical diffusivity of $1\,cm^2/s$ and a Redfield ratio of C:P=106:1. The maximum upward flux of $2\,mol\,C/m^2/a$ corresponds to $8\,Pg\,C/a$ which is close to the estimate of SIEGENTHALER AND SARMIENTO (1993) ($10\,Pg\,C/a$).

that the only pathway of deep water back to the surface is diffusion. So in their framework this diffusivity is the sole process preventing the deep ocean from filling up with cold water sinking at the poles). In 40 m the carbon flux is maximal upwards causing a flux divergence below. This flux divergence must be balanced by remineralization of organic material sinking below 40 m (implicitly assuming that the diffusive flux divergence is not balanced by convergent advection of carbon). This back-of-the-envelope calculation yields a global biotically induced vertical carbon flux of $8\,Pg\,C/a$ which is close to estimates based on more sophisticated approaches (e.g. SIEGENTHALER AND SARMIENTO (1993), $10\,Pg\,C/a$ corresponding to $30\,g\,C/m^2/a$). It is this flux which controls an organic stock of $700\,Pg\,C$ in the deep ocean (for reference: $770\,Pg\,C$ are in today's atmosphere). Changes of this flux (i.e. of the "biological pump") result in a modified oceanic organic and eventually inorganic carbon stock subsequently affecting atmospheric CO_2 concentrations. In its magnitude it is comparable to anthropogenic emission of CO_2 ($6.4\,Pg\,C/a$ fossil fuel combustion in 2001).

As noted already a comprehensive understanding of the "biological pump" enabling us to forecast its behavior in a changing climate has not been achieved yet. Aggravating in that respect is the high temporal and spacial variability of biotic processes which mirror the physical processes controlling the availability of light and essential nutrients. For example, satellite observations reveal high concentrations of surface chlorophyll associated with deep winter mixing bringing nutrients back into the sun-lit surface ocean in subpolar regions and with upwelling off West Africa, America and along the equator.

The focus of the publications submitted here in support of my "Dissertation" ,however, is on the subtropical gyre of the North Atlantic, a vast region, where

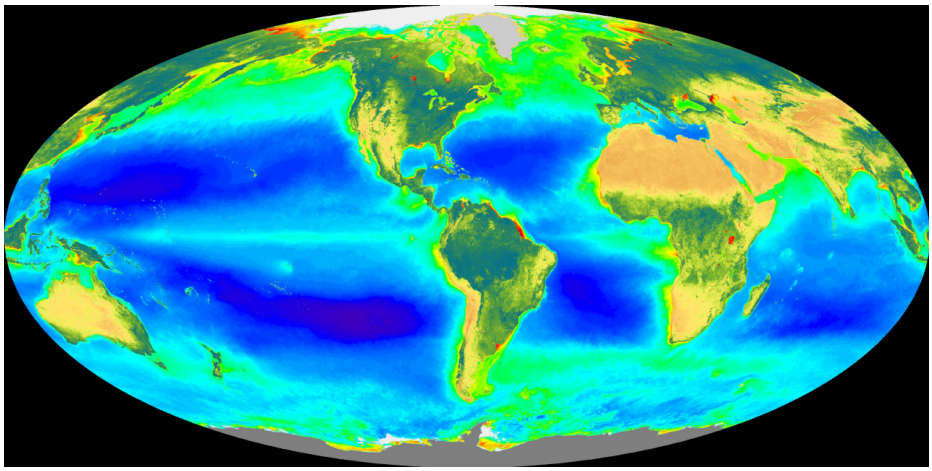

Figure 0.2: Composite image of oceanic chlorophyll concentrations as viewed from space in arbitrary units. Green contours denote high values while blue contours refer to low values. (Obtained through the SeaWifs homepage http://seawifs.gsfc.gov/SEAWIFS.)

chlorophyll concentrations are lowest (Fig. 0.2). Traditionally this region is regarded as an oceanic "desert" where wind stress generated downwelling and shallow winter mixing confine upward nutrient transport to the sun-lit euphotic surface ocean (which in steady state should equal export production of organic material (Eppley and Peterson (1979))). This picture was confirmed by local measurements of turbulent nutrient supply to the euphotic zone and from $^{15}NO_3$ incubations corresponding to an export of only $4\,\mathrm{g\,C/m^2/a}$ (Lewis et al. (1986)).
The enigma this study sets out to resolve is that, on the other hand, measurements of vertically integrated oxygen consumption rates yield an export of organic matter of $47\,\mathrm{g\,C/m^2/a}$ (Jenkins (1982)) which is more than one order of magnitude higher. (Note that irrespective of these estimates even the direction of the biotically effected air-sea flux of carbon is discussed controversely in the region (Duarte and Agusti (1998)), Williams (1998), del Giorgio and Duarte (2002)).) Several reasons for this apparent discrepancy are considered here. The individual research papers are:

- Dietze, H. and A. Oschlies and P. Kähler, 2004: Internal-wave-induced and double-diffusive nutrient fluxes to the nutrient-consuming surface layer in the oligotrophic subtropical North Atlantic. *Ocean Dynamics*, **54**, doi: 10.1007/s10236-003-0060-9.

  - Reexamines nutrient supply to the upper ocean by turbulent mixing using local local standard oceanographic measurements and high-resolution vertical profiles of nutrients averaged over a large region directly comparable to that investigated by Jenkins (1982).

Previously unaccounted nutrient transport into the nutrient-consuming surface layer by salt fingering is found to be more than fivefold higher than transport due to internal-wave induced turbulence. Still, this cannot resolve the above mentioned apparent discrepancy, even if additional physical transport mechanisms such as eddy pumping, advection and horizontal diffusion are accounted for.
Observed NO_3/PO_4 turbulent flux ratios of up to 23 are interpreted as the imprint of N_2 fixation.

- OSCHLIES, A. and H. DIETZE and P. KÄHLER, 2003: Salt-finger driven enhancement of upper ocean nutrient supply. *Geophys. Res. Lett.* , **30**, doi: 10.1029/2003GL018552.

  – By reducing the potential energy of an unstable salinity profile, salt-fingering can, besides internal waves excited by wind and tides, generate turbulent vertical mixing. This study, based on a coupled 3-D eddy-permitting biogeochemical model of the North Atlantic, examines the potential contribution of salt-finger induced mixing to upper-ocean nutrient supply. Due to sparse observational data this is, up-to-date, the only method to exclude that the apparent discrepancy between nutrient supply to and export from the euphotic zone in the oligotrophic subtropical North Atlantic is caused by different scales of time and space in the respective studies (JENKINS (1982), DIETZE ET AL. (2004)).

- DIETZE, H. and A. OSCHLIES, 2004: Modeling abiotic production of apparent oxygen utilisation in the oligotrophic subtropical North Atlantic. *Ocean Dynamics*, submitted.

  – The export estimate of JENKINS (1982), which is based on oxygen consumption rates at depth implicitly assumes that apparent oxygen utilisation is solely effected by biotic processes (i.e. net respiration). Using a coupled 3-D circulation-oxygen model the potential of abiotic, physical processes biasing apparent oxygen utilisation as well as its rates is investigated. Results indicate that the JENKINS (1982) estimate is indeed biased high by O(10%) due to abiotic processes feigning respiration on respective isopycnals. Vertical integration, however, yields an abiotic fraction of less than 3%, so the apparent observational discrepancy can not be resolved.

- KÄHLER, P. and A. OSCHLIES and H. DIETZE and B. MOURINO and M. SANDOW and U. STRUCK, 2004: High rates of nitrogen fixation and DOC subduction in the subtropical North Atlantic Ocean. to be re-submitted.

  – Examines the potential of biological processes previously unaccounted to reconcile the hitherto enigmatic mismatch between organic-matter production and nitrate supply in the subtropical North Atlantic Ocean.

$^{15}N_2$ and $^{14}CO_2$ uptake experiments as well as measurements of dissolved organic carbon and apparent oxygen utilisation in a region directly comparable to that investigated by JENKINS (1982) indicate that N_2 fixation and shallow export of dissolved organic carbon by subduction finally explaines the apparent discrepancy this study set out to resolve.

Results presented in the publications, listed above indicate that the apparent discrepancy is reduced by 20% if additional physical transport mechanisms of nitrate supply to the surface layer and abiotic production of apparent oxygen utilisation at depth are accounted for. The remaining 80% are ascribed to nitrogen fixation and subduction of dissolved organic carbon. In total, the gap we set out to explain is "overexplained" by ca. 15%.
In addition a caveat concerning a standard method used to distinguish between physically and biotically effected air-sea fluxes of oxygen is reported. Measurement accuracy of net air-sea oxygen fluxes is increasing. Along comes an increased temptation to use these fluxes to derive net biotically effected air-sea fluxes of oxygen (which can, using Redfield stoichiometry, be transferred into biotically effected carbon export into the deep ocean). Model results indicate that the standard method, if applied regionally, might well propose the wrong direction of biotically effected carbon export into the deep ocean.

- DIETZE, H. and A. OSCHLIES, 2004: Separating physically and biotically effected air-sea flux of O_2 in the North Atlantic. An easy task? *J. Geophys. Res.*, submitted.

  - Neglecting all mechanisms potentially producing deviations from saturation of a gas dissolved in seawater results in a tight coupling between air-sea heat flux and gas flux. This coupling, or correlation is the standard method to estimate abiotically effected air-sea fluxes of gases with fast air-sea gas exchange such as e.g. oxygen. This study examines the potential of abiotic processes other than finite gas exchange violating the air-sea heat flux to oxygen flux correlation. Based on results from a coupled eddy-permitting 3-D circulation-oxygen model of the North Atlantic two processes are identified:
    (1) Solar radiation penetrating below the mixed layer warms water in spring/summer. As the water warms solubility increases and, since it is shielded from the atmosphere, oversaturation evolves. During autumn/winter, when the mixed layer deepens due to destabilizing surface buoyancy fluxes the oversaturated water gets back into contact with the atmosphere. The net effect is that the standard method yields annual cycles of air-sea oxygen flux biased high as much as 20% to 50% in the subtropical North Atlantic.
    (2) Due to the nonlinear relationship between oxygen saturation (i.e. solubility) and temperature, mixing of two water parcels with different

temperatures and salinities does always result in a mixed parcel oversaturated relative to the mean of the original parcels. Wherever such a water parcel which was subject to intense mixing gets into contact with the atmosphere its oversaturation decouples the oxygen-to-heat flux correlation.

Perspectives

We set out to resolve an apparent inconsistency between estimates of biotically-effected carbon export inferred from vertically integrated oxygen consumption rates (JENKINS (1982); $47\,\mathrm{g\,C/m^2/a}$) in subsurface waters and local measurements of turbulent nutrient supply to the euphotic zone (LEWIS ET AL. (1986); $4\,\mathrm{g\,C/m^2/a}$) in the eastern subtropical North Atlantic. Processes listed in the respective papers of the previous section "overexplain" the apparent discrepancy between the two estimates by ca. 15%. Preliminary results based on a coupled 3-D eddy-permitting biogeochemical model of the North Atlantic indicate that this "overexplanation" is not just an artefact of the errors associated with each estimate:

JENKINS (1982) measured apparent oxygen utilisation, tritium and ^{3}He on isopycnals within the so-called Beta Triangle (Fig. 0.5, named after the beta-spiral method applied to hydrographic section data (STOMMEL AND SCHOTT (1977))). Least-square linear regression between apparent oxygen utilisation and age, derived from the transient tracer pair, yielded oxygen utilisation rates. These oxygen utilisation rates were vertically integrated and converted into an average export of organic matter from the surface ocean using Redfield stoichiometry (see also Fig. 0.3 for further explanation).

In the following this method is assessed in an extended version of the eddy-permitting biogeochemical ocean model used also in OSCHLIES ET AL. (2003). The extensions are an additional oxygen compartment coupled to nitrate fluxes with a fixed Redfield ratio and an age tracer which counts up time in every grid box, except at the surface where age is continuously reset to zero.

In the model it is possible to compare the oxygen utilisation rates estimated with the method described above with the actual remineralisation rates simulated (Fig. 0.4). Applying the method of JENKINS (1982) to model output results in estimates of oxygen utilisation biased low. This is aggravated by the fact that the abiotic fraction caused by abiotic processes explained in DIETZE AND OSCHLIES (subm. 2004a) would, taken alone, lead to an overestimation. Note that the same result is obtained when, instead of using the age tracer, trajectories of artificial drifters are calculated backwards in time in order to calculate the time elapsed since the respective (model) water parcels were in contact with the atmosphere (see also Fig. 0.5).

The artificial drifter trajectories are of additional benefit as they indicate that only $\approx$50% of the water found in the thermocline of the Beta Triangle region stems from

the North and was subducted recently (see also Fig. 0.6). The remaining fraction is of relatively high South Atlantic Central Water (SACW) content which follows at first the circulation around the subtropical gyre and is finally injected from the North into the region of interest. This entrainment of SACW with a high apparent oxygen utilisation (AOU) signal accumulated during a time considerably longer than the few decades which could be resolved with the helium tritium method pushes the isopycnal AOU gradients into a direction that opposes the effect of respiration. At the same time, its effect on the distribution of age on isopycnals is not influenced to the same extent because the water is too old to carry a significant tritium/helium signal. The net effect results in estimates of apparent oxygen utilisation rates (obtained by applying the method of JENKINS (1982)) biased low relative to biotic respiration which actually took place.

Summing up, we can state that: (1) The mismatch between etimates of nitrate supply to the surface layer and oxygen utilisation at depth in the oligotrophic subtropical North Atlantic is reduced by 20% if physical processes previously neglected are accounted for. (2) The remaining 80% are ascribed to biogeochemical processes, namely nitrogen fixation and subduction of dissolved organic carbon (DOM). (3) To the extent that the model circulation is correct, the estimate of apparent oxygen utilisation rates by JENKINS (1982) might be a lower limit i.e. biogeochemical processes might play an even more vital role than revealed in this thesis.

Concerning the previous point it is obviously crucial to explore the extent the physical circulation model can be trusted with respect to its capability of reproducing the circulation and (diffusive) water-mass transformation in the subtropics. Unfortunately, the assessment of circulation and diffusion in general ocean circulation models is not trivial (and was beyond the scope of this thesis), inter alia because it has to include a comprehensive understanding of spurious numerical effects caused by advection and (biharmonic) diffusion schemes (e.g. DIETZE AND OSCHLIES (subm. 2004b)). Nevertheless it has to precede a mechanistical understanding of N_2 fixation and DOM production/consumption since, due to sparse observational data, biogeochemical general ocean circulation models provide, until now, the only platform to constrain the effect of these biotic processes on basin scale.

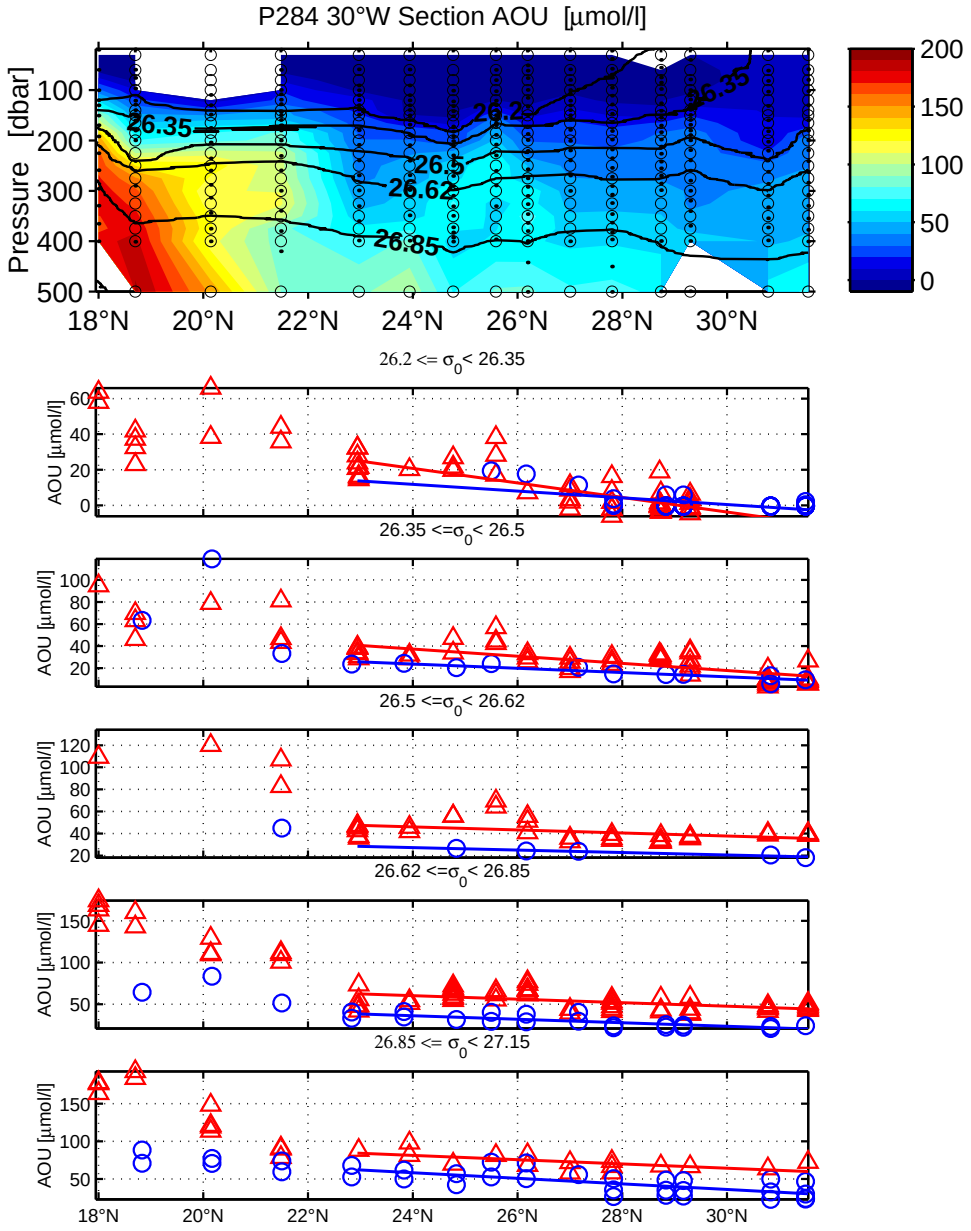

Figure 0.3: *Upper panel: Meridional transect of apparent oxygen utilisation (AOU) observed along 30° W. Black, labeled contours refer to density σ_0. Black dots denote observations, circles are supporting points obtained by vertical linear interpolation of observations prior to contouring. Following an isopycnal from North to South reveals increasing AOU. The lower panels emphasise this distribution for respective density classes (red triangles).* Jenkins *(1982) combined this information with information of time elapsed since the respective water parcels were in contact (and equilibrium as regards their oxygen saturation) with the atmosphere and obtained positive apparent oxygen utilisation rates since age increases southwards with extended distance from the subduction sites in the North. The abrupt increase in AOU south of 24° N is related to a sudden increase of relatively old South Atlantic Central Water content (*Dietze et al. *(2004)). Blue circles denote modeled AOU for reference.*

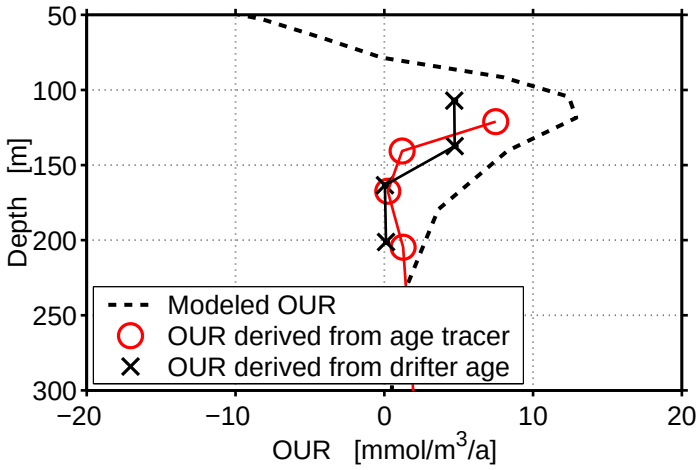

Figure 0.4: *Modeled oxygen utilisation (OUR) by remineralisation and OUR estimated by applying the method of* Jenkins *(1982) to model output using two different "clocks".*

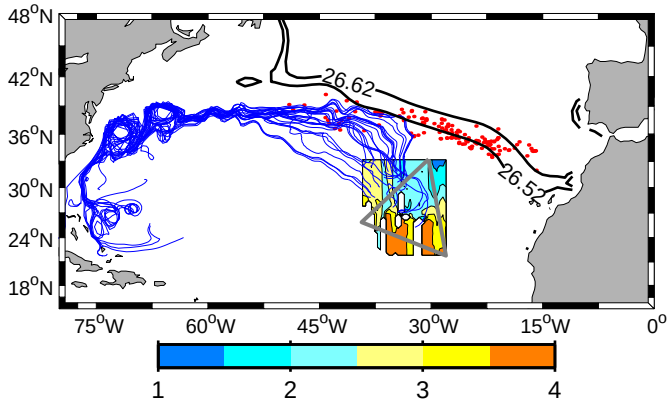

Figure 0.5: *Drifter trajectories calculated backwards in time. Artificial drifters were deployed in the model on respective isopycnals (here an example for* $\sigma_0 = 26.62$*) within the (grey) Beta Triangle. The time it took them to reach the surface mixed layer is denoted by the color scale of the respective trajectory end points in the Beta Triangle region (units are years). Red dots denote the positions where the drifters reached the mixed layer. Only* $\approx$*50% of all drifters deployed reached the surface near the outcrop positions proposed by the climatologies of* Levitus and Boyer *(1994) and* Levitus et al. *(1994) (black, labeled contours). The remaining fraction of drifters deployed did not reach the surface mixed layer within more than 20 years. Their pathways are exemplariliy denoted by blue lines.*

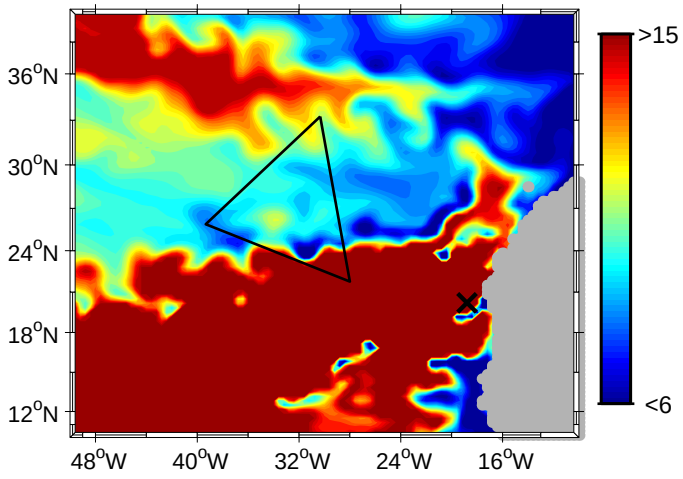

Figure 0.6: *Modeled concentration of an artificial tracer (arbitrary units) on* $\sigma = 26.62$ *after 24 years of integration. The tracer was continuously released at the site marked with a black cross situated south of the Cap Verde Frontal Zone where South Atlantic Central Water content is high. Apparently, entrainment from the North provides an effective pathway of SACW into the (black) Beta Triangle Region.*

Bibliography

Archer, D. E., G. Eshel, A. Winguth, W. Broecker, R. Pierrehumbert, M. Tobis and R. Jacob, 2000: Atmospheric pCO_2 sensitivity to the biological pump in the ocean. *Global Biogeochem. Cycles*, **4**, p. 1219–1230.

Broecker, W. S. and T. H. Peng, 1998: *Greenhouse Puzzles*. 2nd ed.; Lamont-Doherty Earth Observatory of Columbia University: Palisades, NY.

Conkright, M. E., S. Levitus and T. P. Boyer, 1994: World Ocean Atlas 1994. Volume 1: Nutrients. Noaa atlas nesdis 1, NOAA, Washington D.C.

Crawley, T., 1995: Ice age terrestrial carbon changes revisited. *Global Biogeochem. Cycles*, **9**, p. 377–389.

del Giorgio, P. A. and C. M. Duarte, 2002: Respiration in the Open Ocean. *Nature*, **420**, p. 379–384.

Dietze, H. and A. Oschlies, subm. 2004a: Modeling abiotic production of apparent oxygen utilisation in the oligotrophic subtropical North Atlantic. *Ocean Dynamics*.

Dietze, H. and A. Oschlies, subm. 2004b: Seperating physically and biotically effected air-sea flux of O_2 in the North Atlantic. An easy task? *Journal of Geophysical Research*.

Dietze, H., A. Oschlies and P. Kähler, 2004: Internal-wave-induced and double-diffusive nutrient fluxes to the nutrient-consuming surface layer in the oligotrophic subtropical North Atlantic. *Ocean Dynamics*, **54** (1), p. doi: 10.1007/s10236–003–0060–9.

Duarte, C. M. and S. Agusti, 1998: The CO_2 Balance of Unproductive Aquatic Ecosystems. *Science*, **281**, p. 234–236.

Eppley, R. W. and B. J. Peterson, 1979: Particulate organic matter flux and planktonic new production in the deep ocean. *Nature*, **282**, p. 677–680.

Jenkins, W. J., 1982: Oxygen utilisation rates in the North Atlantic subtropical gyre and primary production in oligotrophic systems. *Nature*, **300**, p. 246–248.

Levitus, S. and T. P. Boyer, 1994: World Ocean Atlas 1994. Volume 4: Temperature. Noaa atlas nesdis 4, NOAA, Washington D.C.

LEVITUS, S., R. BURGETT and T. P. BOYER, 1994: World Ocean Atlas 1994. Volume 3: Salinity. Noaa atlas nesdis 3, NOAA, Washington D.C.

LEWIS, M. R., G. HARRISON, N. S. OAKEY, D. HERBERT and T. PLATT, 1986: Vertical nitrate fluxes in the oligotrophic ocean. *Science*, **234**, p. 870–873.

MUNK, W. and C. WUNSCH, 1998: Abyssal recipes II: energetics of tidal and wind mixing. *Deep-Sea Res.*, **45**, p. 1976–2009.

OSCHLIES, A., H. DIETZE and P. KÄHLER, 2003: Salt-finger driven enhancement of upper ocean nutrient supply. *Geophys. Res. Lett.*, **30**, p. doi: 10.1029/2003GL018552.

SHIMEL, D., I. G. ENTING, H. HEIMANN, T. M. L. WIGLEY, D. RAYNAUD, D. ALVES and U. SIEGENTHALER, 2001: *in Climate Change 1994 (ed. Houghton, J.T.)*. Cambridge Univ. Press.

SIEGENTHALER, U. and J. L. SARMIENTO, 1993: Atmospheric carbon dioxide in the ocean. *Nature*, **365**, p. 119–125.

SIGMAN, D. M. and E. A. BOYLE, 2000: Glacial/interglacial variations in atmospheric carbon dioxide. *Nature*, **407**, p. 859–869.

STOMMEL, H. and F. SCHOTT, 1977: The Beta Spiral and the determination of the absolute velocity field from hydrographic station data. *Deep-Sea Research*, **24**, p. 325–329.

WATSON, R. T. and D. L. ALBRITTON, 2001: *Climate change 2001: Synthesis report*. Cambridge; New York: Cambridge University Press.

WILLIAMS, P. J. L. B., 1998: The Balance of Plankton Respiration and Photosynthesis in the Open Oceans. *Nature*, **394**, p. 55–57.

Internal-wave-induced and double-diffusive nutrient fluxes to the nutrient-consuming surface layer in the oligotrophic subtropical North Atlantic

H. Dietze, A. Oschlies and P. Kähler, 2004
Published in Ocean Dynamics

Ocean Dynamics (2004) 54: 1–7
DOI 10.1007/s10236-003-0060-9

Heiner Dietze · Andreas Oschlies · Paul Kähler

Internal-wave-induced and double-diffusive nutrient fluxes to the nutrient-consuming surface layer in the oligotrophic subtropical North Atlantic

Received: 20 December 2002 / Accepted: 13 June 2003

Abstract In the literature, an inconsistency exists between estimates of biotically-effected carbon export inferred from large-scale geochemical studies (Jenkins 1982; 47 gC m^{-2} a^{-1}) and local measurements of turbulent nutrient supply (Lewis et al. 1986; 4 gC m^{-2} a^{-1}) in the eastern subtropical North Atlantic. Nutrient supply to the upper ocean by turbulent mixing is reexamined using local standard oceanographic measurements and high-resolution vertical profiles of nutrients averaged over a large region directly comparable to that investigated by Jenkins (1982).

Turbulent fluxes induced by internal waves and salt fingering, respectively, are separated according to Gregg (1989) and Zhang et al. (1998). Nutrient transport into the nutrient-consuming surface layer by salt fingering is more than fivefold higher than transport due to internal-wave induced turbulence. Still, this cannot resolve the above-mentioned apparent inconsistency, even if additional physical transport mechanisms such as eddy pumping, advection and horizontal diffusion are accounted for. Estimated nitrate fluxes due to vertical turbulent diffusion are 0.05–0.15 mol m^{-2} a^{-1}, corresponding to 4–11 gC m^{-2} a^{-1}. Observed NO_3/PO_4 turbulent flux ratios of up to 23 are interpreted as the imprint of N_2 fixation.

Keywords Nutrient transport · Salt fingering · Double-diffusive fluxes

1 Introduction

A method to estimate the export of organic matter from the surface ocean is to vertically integrate oxygen consumption rates in subsurface waters. Jenkins (1982) applied this in the so-called Beta Triangle (named after the beta-spiral method applied to hydrographic section data (Stommel and Schott 1977) in the subtropical North Atlantic (Fig. 1). It yielded an average export corresponding to 0.63 mol Nm^{-2} a^{-1} (using a $-O_2 : N = 9.1$ ratio following Minster and Boulahdid 1987).

Lewis et al. (1986) quantified new production, which in steady state should equal export production (Eppley and Peterson 1979), from $^{15}NO_3$ incubations and estimates of the diffusive nitrate supply at a site nearby (Fig. 1). When taken as representative of a whole year, their new production estimate amounts to only 10% of the export estimate of Jenkins (1982).

Several reasons for this apparent discrepancy can be considered, among them: (1) different scales of time and space in the two respective studies, (2) nitrogen sources other than nitrate (N_2 fixation, dissolved organic nitrogen, atmospheric deposition), (3) export of organic matter high in C (dissolved organic carbon, hereafter named DOC), (4) vertically migrating organisms influencing the nutrient and oxygen distributions and (5) lateral entrainment of low-oxygen water feigning local oxygen consumption. However, also the physical transport mechanisms of nitrate supply to the surface are arguable. As Hamilton et al. (1989) suggested, the Lewis et al. (1986) estimate may be too low by up to a factor of 6 due to the neglect of salt fingering. By reducing the potential energy of an unstable salinity profile, salt fingering can, besides internal waves excited by wind and tides, generate turbulent vertical mixing.

The region and depth of interest (Central Water, pycnocline of the subtropical gyre) was described as having a strong double-diffusive potential already by Ingham (1966). The problem ever since has been the quantification of double-diffusive fluxes. Attempts based on laboratory experiments (Turner 1965, 1967), suffered from limited portability to open-ocean conditions where the growth of salt fingers is suppressed by inertial shear (Kunze 1987) and internal-wave-induced turbulence (Marmorino 1990), which are difficult to simulate in the laboratory.

Responsible Editor: Franciscus Colijn

H. Dietze · A. Oschlies · P. Kähler
Institut für Meereskunde, Kiel
e-mail:hdietze@ifm.uni-kiel.de

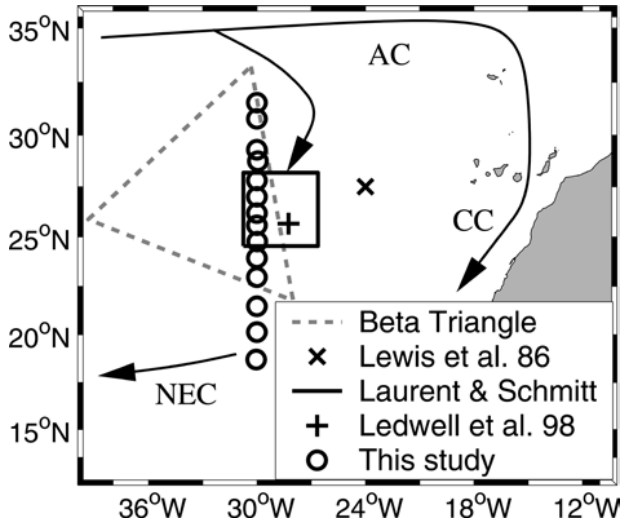

Fig. 1 Locations of this and related studies. *Circles* denote positions of CTD-Rosette casts. *Arrows* sketch the pathways of Azores Current (*AC*), Canary Current (*CC*) and North Equatorial Current (*NEC*) according to a compilation of near-surface drifters by Brügge (1995)

A relatively new approach is the quantification of salt-finger fluxes based on microstructure measurements. As Hamilton et al. (1989) noted, there is an uncertainty in diffusivities inferred from microstructure of almost 1 order of magnitude depending on whether the source of observed turbulence was salt-fingering or internal waves. Laurent and Schmitt (1999) developed a model which can distinguish between the signatures of internal-wave-induced turbulence and salt fingering. Their application of the model to the NATRE (North Atlantic Release Experiment) microstructure data was consistent with diffusivities inferred from the spreading rates of a released tracer (Ledwell et al. 1998). Laurent and Schmitt (1999) also computed dianeutral velocities based on profiles of density and microstructure-inferred diffusivities for salt and heat. The result was in good agreement with the observed downward movement of the tracer's centre of mass relative to the isopycnal surface at which the tracer had been injected. This gives confidence to their estimate of double-diffusive fluxes because the dianeutral velocity is a function of the salt-to-density flux ratio (McDougall 1987).

In our study, internal-wave- and salt-finger-induced diffusivities are scaled using standard oceanographic measurements (CTD, VM-ADCP) taken in the Beta Triangle region. In order to assess the quality of the parameterizations used, the results are compared with estimates of Laurent and Schmitt (1999) at the NATRE site which is overlapping the Beta Triangle (Fig. 1). Net nutrient supply into the surface layer is quantified by combining diffusivities with high-resolution vertical nutrient profiles and accounting for Ekman pumping, dianeutral velocities as well as horizontal nutrient fluxes as recommended by McDougall and Ruddick (1992). Using Redfield stoichiometry and assuming steady state, upward nutrient fluxes are converted into export of organic material. This allows a direct comparison with the earlier estimate by Jenkins (1982) based on oxygen utilization rates at depth.

This study examines the potential of salt-fingering (double diffusion) to close the apparent dicrepancy between biotically generated carbon export from, and nitrate supply to, the surface layer of the study area.

2 Data

Data were obtained during an FS Poseidon Cruise (March 10–22, 2002) along 30°W (18°N–31.5°N) (Fig. 1).

Horizontal velocities in the upper ocean were continuously measured with a 150-kHz narrow-band acoustic Doppler current profiler (VM-ADCP, RD Instruments) mounted into the ship's hull. The device yielded ensemble-averaged velocity profiles in 8-m depth bins every 3 min. One ensemble consisted of 150 profiles. Low concentration of scattering particles within the extremely oligotrophic environment restricted the quantitatively reliable range to about 250 m.

CTD casts were taken at a spatial resolution of about 27 nautical miles down to a depth of 2000 m. The MARK III conductivity–temperature–depth instrument was fitted with a fluorometer, measuring the fluorescense of chlorophyll-a, and a Rosette sampler system.

Nutrient concentrations were measured by standard procedures (Grasshoff et al. 1983). Obtained accuracy was ± 0.1 mmol m^{-3} and ± 0.02 mmol m^{-3} for nitrate and phosphate, respectively. In this study "nitrate" refers to the sum of nitrate and nitrite. A few measurements of ammonium showed negligible concentrations and are not included in our nutrient budget. Reference measurements of salinity with a laboratory salinometer (Autosal) during the cruise showed CTD salt measurements to be accurate within ± 0.003 PSU. Pre- and postcruise calibration of the temperature probe proposed an absolute accuracy of ± 0.005 K for temperature measurements. Resolution, relevant for computing gradients, was assessed as proposed by the manufacturer with ± 0.0005 K and ± 0.001 PSU for temperature and salinity, respectively. Assuming that temperature and salinity errors are uncorrelated, error propagation yields a signal-to-noise ratio of at least 10 for the fourth moment of stability frequency, N^4, in the stratified thermocline.

The VM-ADCP data were calibrated using the CODAS 3 software package of Firing (2001). Sound speed in the vicinity of the pinger was calculated with spatially interpolated CTD data. Absolute velocity errors of a single ensemble are of O(5 cm s^{-1}), mainly due to the inaccuracy of satellite navigation and randomly distributed around a mean, real value. Relative velocity errors σ_v as relevant to the estimation of vertical shear are calculated as proposed by the manufacturer:

$$\sigma_v = 1.6 \times 10^5 / \left(FD\sqrt{N} \right) \ , \qquad (1)$$

with pinger's frequency $F = 150$ kHz, depth bin $D = 8$ m and number of measurements $N = 150$ within a 3-min ensemble. This yields $\sigma_v = 1$ cm s^{-1}.

3 Inferring diffusivities

3.1 Methods

3.1.1 Internal-wave-induced diffusivities

The dissipation rate of turbulent kinetic energy ϵ_{iw} fed by the loss of energy of the internal wave field was scaled according to Gregg (1989) as a function of the local buoyancy frequency N and variance of shear S_{10}^2 contributed by vertical wavelengths greater than 10 m. Combination with the relationship of Osborn (1980), who proposed the upper bound of diapycnal diffusivity of density K_{iw} to be a function of N and ϵ_{iw} only, yields:

$$K_{iw}(z) \leq K_0 \left\langle \frac{S_{10}^4}{N^4} \right\rangle \ , \tag{2}$$

(form adopted from D'Asaro and Morison 1992), where angular brackets denote average over space or time and $K_0 = 5 \times 10^{-6}\,\mathrm{m^2 s^{-1}}$, is a constant identical to the formulation of Gregg (1989).
The local buoyancy frequency was calculated according to:

$$N = \sqrt{\frac{-g}{\rho}\frac{\partial \rho}{\partial z}} \ , \tag{3}$$

where the density gradient was estimated from CTD data using least-squares linear regressions over 8-m depth bins.

The fourth moment of vertical shear variance was calculated from the vessel-mounted ADCP data as

$$\langle S_{10}^4 \rangle = \left\langle \left\{ C \left[\left(\frac{\Delta u}{\Delta z} \right)^2 + \left(\frac{\Delta v}{\Delta z} \right)^2 \right] \right\}^2 \right\rangle \ , \tag{4}$$

where $C = 2.54$ is a correction factor adopted from Wijesekera et al. (1993). This correction accounts for both finite differencing at $\Delta z = 8$ m and for the ADCP trapezoidal filter applied to the velocity estimates prior to finite differencing. Trapezoidal filtering is a consequence of the acoustic measurement principle as finite acoustic pulse lengths and return gate widths are required to calculate Doppler shifts.

Angle brackets in Eq. (4) indicate an ensemble average over 200 profiles corresponding to 10 h in time and approximately 50 nautical miles in space. Ensemble means of 200 profiles were chosen as a trade off between a short averaging period and matching the precondition

$$\langle S_{10}^4 \rangle = 2 \langle S_{10}^2 \rangle^2 \ , \tag{5}$$

which is recommended for the application of the scaling (Gregg 1989).

ADCP shear estimates are biased as a consequence of the measurement principle (Polzin et al. 2002). Relevant for VM-ADCP measurements are range-averaging and finite differencing which are taken into account by the factor C in Eq. (4), vertical averaging of horizontally non-uniform currents due to the effect of beam separation with increasing depth, effect of instrument noise σ_v and tilting or instrument inclination which is thought to be a minor effect considering the relatively calm conditions during the cruise. Alford and Pinkel (2000) propose that an overly pessimistic estimate of the upper bound of the effect of beam separation is an underestimation of S_{10}^2 by 60% at most. Due to uncertainties of this estimate, data in this study are not corrected for the latter effect. Noise biases S_{10}^2 high by $2\sigma_v^2/(\Delta z)^2$. This is accounted for by substracting this bias from estimates of $\langle S_{10}^4 \rangle$. The scaling itself (Eq. 2) is uncertain within a factor of 2 (Gregg 1989).

3.1.2 Salt-fingering-induced diffusivities

"It is generally agreed that the diffusivity of salt due to salt fingers equals the diffusivity of mineral nutrients because of similar molecular characteristics of mineral nutrients and other major ions which constitute the salt content of seawater" (Hamilton et al. 1989). Following Schmitt (1981), the diffusivity of salt and nutrients due to salt fingering, K_s, was parameterized as a function of the local density ratio $R_\rho = \alpha T_z / \beta S_z$ as:

$$K_s = \frac{K^\star}{1 + \left(R_\rho / R_c \right)^n} \ . \tag{6}$$

The critical density ratio $R_c = 1.6$, the maximum diapycnal diffusivity due to salt fingers $K^\star = 1.0$ cm^{2}s^{-1} and the index $n = 6$ were all adopted from Zhang et al. (1998), who modified original values in order to be consistent with results from the C-SALT program.

The density ratio $R_\rho(z)$ was calculated from CTD-data using least-squares linear regressions over 15 m depth bins to estimate salt and temperature gradients.

Uncertainties of the scaling are not quite clear, but as herein derived estimates of K_s coincide reasonably with micro structure measurements of Laurent and Schmitt (1999) in the same region (Fig. 3a), we conclude that the scaling is suitable.

3.2 Obtained diffusivities

Within the pycnocline, the upper boundary of which is taken as the mixed-layer depth (Fig. 2), the internal-wave-induced diffusivity K_{iw} varies between 5×10^{-7} m^2 s^{-1} and 5×10^{-5} m^2 s^{-1} without apparent vertical or horizontal structure (Fig. 3b). The meridional mean internal-wave-induced diffusivity reproduces the often-observed "pelagic" value of 1×10^{-5}m^{2}s^{-1} (e.g. Ledwell et al. 1998). Our measurements are well above noise

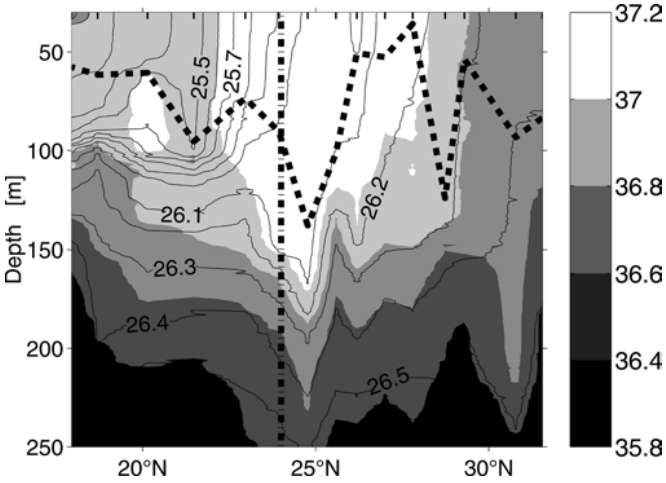

Fig. 2 Meridional section of salinity (*filled contours*) and σ_0 (*labeled contours*) along 30°W. *Dashed line* marks the surface mixed-layer depth, here defined as the depth where temperature is 0.1 K less than SST. South of 24°N (indicated by *vertical dash-dotted line*) water mass analysis based on temperature, salinity and silicate distribution on $\sigma_0 = 26.62$ (corresponding to approximately 270 m depth) showed a sudden increase of South Atlantic Central Water. All budget calculations in this paper refer to the region north of 24°N

level, and significant regional differences in the derived diffusivities should thus be resolved. The meridional dependence of internal-wave-induced diffusivity as suggested by Hibiya et al. (1999) or Gregg (1989) is therefore negligible in the latitude range under investigation.

Turbulent diffusion due to salt-fingering varies between 0 $m^2\ s^{-1}$ and $7 \times 10^{-5}\ m^2\ s^{-1}$ within the pycnocline (Fig. 3c). Its meridional mean at the upper bound of the pycnocline reaches values up to $7.5 \times 10^{-5}\ m^2\ s^{-1}$, which is more than sevenfold higher than the average internal-wave-induced diffusivity in the same depth (Fig. 3a).

Adding up internal-wave- and salt-finger-induced diffusivities (Fig. 3a) results in a total vertical turbulent diffusivity which agrees within error bounds (at least within the pycnocline) with the estimates of Laurent and Schmitt (1999) based on microstructure measurements at the NATRE site.

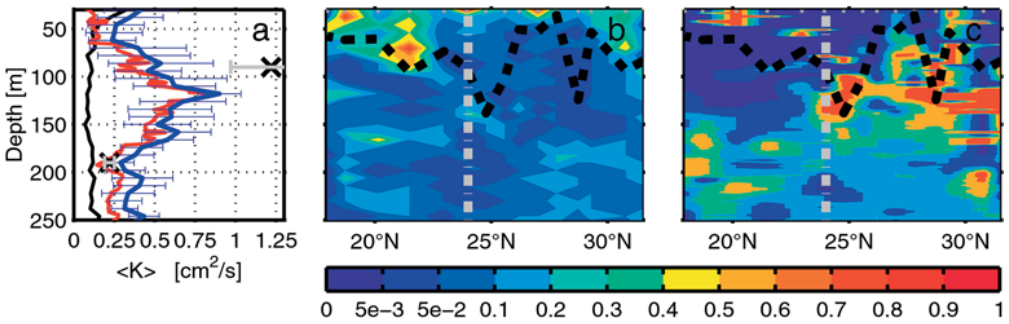

Fig. 3a–c Vertical diffusivities along 30°W. Units are $cm^2\ s^{-1}$. **a** Meridional mean of data north of 24°N. *Black line* is mean of internal-wave induced diffusivity, *red line* is diffusivity due to salt-fingering and *blue line* is the sum of both. *Blue error bars* represent 95% confidence intervals calculated from meridional variance. *Black x-marks* and *grey error bars* are estimates of Laurent and Schmitt (1999). **b** Contour plot of internal-wave- induced diffusivity. *Dashed line* is mixed-layer depth, *dash-dotted line* is at 24°N. **c** Contour plot of turbulent diffusivity due to salt fingering

4 Nutrient fluxes

New production is that share of production which is fuelled by the supply of nutrients from outside the euphotic zone. Hence, when addressing diffusive nitrate supply as the basis of new production, i.e. supply into the euphotic zone, the lower boundary of the euphotic zone needs to be known. Strictly, this is the compensation depth of photosynthesis, which is seldom determined (and may be non-determinable considering the difficulties in distinguishing between gross and net production). In this study we use the depth of maximum upward nitrate transport as the reference depth, which is 20 m below the deep chlorophyll maximum and roughly coincides with the 0.1% light level (Fig. 4b).

According to the monthly climatologies of Levitus et al. (1994) and Levitus and Boyer (1994), this depth level is always beneath the surface mixed layer, within the well-stratified pycnocline, so that nutrient entrainment due to destabilizing surface fluxes need not be considered.

The layer above the maximum upward nitrate transport is termed the nutrient-consuming surface layer rather than the euphotic zone. The relevance of the reference depth used here is that upward diffusive nitrate transport through this depth level causes a flux convergence in the upper part of the water column which, in steady state, must be balanced by consumption and subsequent export of nitrogen contained in organic matter. Note that in this concept there is no distinction between nitrate-removing processes in the surface layer as regards their dependence on light, i.e. dark uptake by vertically migrating algae and heterotrophic nitrate uptake by DOC consumers are included as well as uptake by photosynthetic algae.

Nutrient fluxes F were calculated according to:

$$F = (K_S + K_{iw}) \frac{\partial \mathrm{nut}}{\partial z} \quad , \tag{7}$$

where nut denotes respective nutrient concentrations.

Mean fluxes into the nutrient-consuming layer are 0.1 ± 0.05 mol $m^{-2}\ a^{-1}$ and 4.3 ± 2 mmol $m^{-2}\ a^{-1}$ for nitrate and phosphate, respectively (Fig. 4). Error

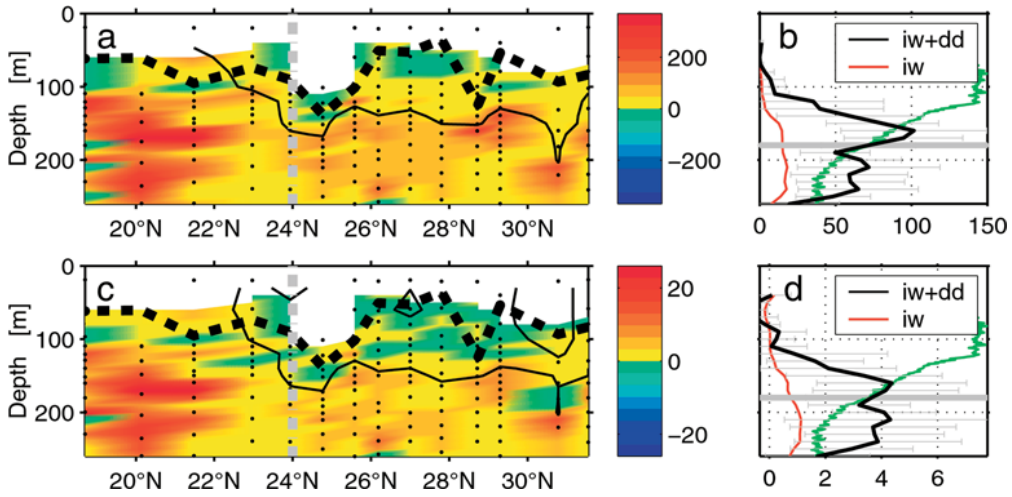

Fig. 4a–d Diffusive NO_3 and PO_4 fluxes. Units are mmol $m^{-2}a^{-1}$. *Positive values* describe upward fluxes. **a** Diffusive NO_3 fluxes along 30°W. *Dashed line* is the surface mixed-layer depth, *black line* is 0.5 mmol NO_3 m^{-3} isoline. South of 24°N (*vertical dash-dotted line*) South Atlantic Central Water content increases rapidly. **b** Meridional mean of diffusive NO_3 fluxes north of 24°N. *Red line* are fluxes due to internal-wave- induced diffusivity, *black line* is the sum of internal-wave- and salt-finger-induced NO_3 fluxes. Error bars indicate 95% confidence intervals calculated from meridional variance. *Grey line* is 0.1% light level, *green line* is fluorosence of chlorophyll-a in arbitrary units. **c** Diffusive PO_4 fluxes along 30°W. *Black line* is 0.03 mmol PO_4 m^{-3}. **d** Meridional mean of diffusive PO_4 fluxes north of 24°N

bounds are 95% confidence intervals calculated from meridional variance. The NO_3:PO_4 flux ratio reaches values up to 23, which is significantly higher than the Redfield N:P ratio of 16 (Fig. 5).

Below the depth of maximum upward nitrate flux the N:P flux ratio decreases to the Redfield ratio within a short distance. This indicates excess nitrate remineralization in the depth range between 140 and 180 m. This layer is provided with N:P in the Redfield ratio from below but looses these nutrients in a much higher N:P ratio to the nutrient-consuming surface layer by diffusive fluxes which are higher in N (Fig. 5). (Note that this result does not depend on the quality of estimates of diffusivities, as the flux ratio is solely a function of respective nutrient gradients.) Particulate organic matter in the surface had a similarly elevated N:P ratio (Kähler et al. (unpublished manuscript)).

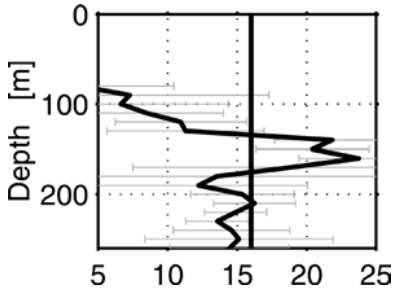

Fig. 5 Meridional mean of diffusive NO_3 and PO_4 flux ratios north of 24°N. *Error bars* are 95% confidence intervals calculated from meridional variance, *vertical black line* indicates the Redfield ratio

5 Discussion

A crucial question is, to what extent the obtained diffusive fluxes can be regarded as total nutrient fluxes into the nutrient-consuming surface layer. Additional physical transport mechanisms other than turbulent vertical diffusion are horizontal and vertical advection, horizontal diffusion and eddy pumping. Results from an eddy-resolving coupled ecosystem-circulation model propose that eddy pumping contributes a nitrate flux of less than 50 mmol m^{-2} a^{-1} to the surface layer in the region under investigation (Oschlies 2002a).

Divergences of horizontal fluxes as well as of vertical advection of NO_3 were calculated for a box meridionally bounded by 24°N and 32°N and zonally bounded by 34.5°W and 25.5°W. Table 1 lists the respective contributions to the budget, which were obtained as follows.

Meridional and zonal divergence of diffusive fluxes were calculated by combining nitrate gradients, derived from the annual Conkright et al. (1994) climatology on scales of 400 km, with a horizontal diffusivity of 1000 m^2 s^{-1} (e.g. Bauer and Siedler 1988).

Meridional and zonal divergences of advective fluxes were calculated by combining the meridional mean of measured VM-ADCP velocities (6.5 cm s^{-1} southward,

Table 1 Budget of NO_3 fluxes within 24°N–32°N, 34.5°W–25.5°W and the upper 160 m. *Negative numbers* define loss of the nutrient-consuming surface layer

Mechanism	mmol NO_3 m^{-2} a^{-1}
Double-diffusive vertical flux	85 ± 44
Internal-wave induced vertical flux	15 ± 7
Zonal convergence of lateral advective flux	4
Meridional convergence of lateral advective flux	38
Zonal divergence of lateral diffusive flux	−5
Meridional convergence of lateral diffusive flux	28
Vertical divergence of vertical advective flux	−73
Uncertainty due to inconsistent volume budget	< 26
Eddy pumping Oschlies (2002a)	< 50
NAO-induced interannual variations Oschlies (2001)	< 50

1.6 cm s^{-1} westward) with nitrate concentrations from the annual Conkright et al. (1994) climatology.

Following McDougall and Ruddick (1992), the vertical velocity w was split into a component parallel to neutral surfaces (which locally follow isopycnals) and a dianeutral one. For the region under investigation, typical Ekman pumping velocities parallel to neutral surfaces are around 31 m a^{-1}. (McClain and Firestone 1993). This downward volume flux must be balanced by horizontally convergent velocities. As the velocities used to obtain estimates of horizontally convergent nitrate fluxes were assumed to be constant within the box used for this budget calculation, this is inconsistent. Assuming Ekman pumping to be balanced by an extra inflow of 0.55 cm s^{-1} from the north only is connected with the largest error (26 mmol m^{-2} a^{-1}) because nitrate concentrations along 32°N are highest relative to the other sides bounding the box.

Dianeutral velocities can be calculated considering a steady-state, quasi-one-dimensional ocean in terms of conservation equations for potential temperature and salinity within a neutral surface framework (McDougall 1991). This concept assumes no density-flux divergences along neutral surfaces (so these velocities need not be balanced by horizontally convergent velocities) and a density field constant in time. Hence, convergences of the vertical diffusive density flux must be balanced by the divergent dianeutral advection of density.

In practice, it is no easy task to estimate dianeutral velocities because second derivatives of vertical profiles of salt, potential temperature as well as internal-wave- and salt-finger-induced diffusivities must be calculated. Here we use the estimate of Laurent and Schmitt (1999) for the NATRE site, who, based on micro structure data from 100 stations, propose a downward dianeutral velocity of 2.96 ± 6.96 m a^{-1} for the depth range 190 ± 50 m. The contribution of vertical advection to the budget (Table 1) was calculated by combining Ekman pumping velocity and dianeutral advection with annual Conkright et al. (1994) nitrate concentrations at the lower boundary of the nutrient-consuming surface layer of the box under consideration.

Summing up, the combined effects of horizontal fluxes and vertical advection yield a loss of 8 ± 26 mmol NO_3 m^{-2} a^{-1} (Table 1). The error is associated, as explained above, with inconsistencies connected with the volume budget. This result coincides with model results of Oschlies (2002b), which suggest that the net effect of advection and horizontal diffusion, as well as their interannual variability induced by the North Atlantic Oscillation (NAO), (Oschlies 2001) is close to zero in the region under investigation.

6 Conclusion

Returning to the apparent discrepancy between nutrient supply and estimated organic-matter export derived from oxygen consumption, described in the Introduction, we can state that:

- Turbulent diffusion due to internal-waves accounts for a nitrate supply of 15 ± 7mmol m^{-2} a^{-1}.
- Turbulent diffusion due to salt-fingering accounts for an additional supply of 85 ± 44 mmol m^{-2} a^{-1}.
- Combined effects of horizontal diffusion, eddy pumping, vertical and horizontal advection add up to an additional supply of less than 50 mmol NO_3 m^{-2} a^{-1}.
- This upward revision of total nitrate supply to the surface layer of 150 mmol m^{-2} a^{-1} corresponding to an export of 11 gC m^{-2} a^{-1} does not resolve the nutrient supply-versus-export discrepancy. Even the upper bound of this estimate (270 mmol NO_3 m^{-2} a^{-1}), obtained by summing up all uncertainties is below the lower bound (480 mmol NO_3 m^{-2} a^{-1})) of the Jenkins (1982) estimate, so the other possibilities of the reconciliation between nutrient supply and oxygen consumption remain to be examined.

The marked deviation from the canonical Redfield ratio of turbulent N:P fluxes to and from the surface layer points to a near-surface N source, probably N_2 fixation, which was shown to produce particulate organic matter of elevated N:P ratios (Karl et al. 1992). This, and the export of nitrogen-poor dissolved organic matter were shown to finally resolve the discrepancy by Kähler et al. (unpublished manuscript).

Acknowledgements We acknowledge constructive comments by the anonymous referees and funding by the Deutsche Forschungsgemeinschaft. Nutrients were measured by Kerstin Nachtigall.

References

Alford MH, Pinkel R (2000) Observations of overturning in the thermocline: the context of ocean mixing. J Phys Oceanogr 30: 805–832

Bauer E, Siedler G (1988) The relative contributions of advection and isopycnal and diapycnal mixing below the subtropical salinity maximum. Deep-Sea Res 35(5A): 811–837

Brügge B (1995) Near-surface mean circulation and kinetic energy in the central North Atlantic from drifter data. J Geophys Res 100(C10): 20543–20554

Conkright ME, Levitus S, Boyer TP (1994) World ocean atlas 1994, vol. 1. Nutrients. Noaa atlas nesdis 1, NOAA, Washington DC

D'Asaro EA, Morison JH (1992) Internal waves and mixing in the Arctic Ocean. Deep-Sea Res 39(2): 459–484

Eppley RW, Peterson BJ (1979) Particulate organic matter flux and planktonic new production in the deep ocean. Nature 282: 677–680

Firing E (2001) CODAS 3 software package for ADCP data. www.moli.soest.hawaii.edu/software/codas3

Grasshoff K, Ehrhardt M, Kremling K (1983) Methods of seawater analysis. Verlag Chemie, Weinheim

Gregg MC (1989) Scaling turbulent dissipation in the thermocline. J Geophys Res 94: 9686–9698

Hamilton JM, Lewis MR, Ruddick BR (1989) Vertical fluxes of nitrate associated with salt fingers in the worlds oceans. J Geophys Res 94: 2137–2145

Hibiya T, Nagasawe M, Niwa Y (1999) Model predicted distribution of internal wave energy for diapycnal mixing processes

in the deep waters of the North Pacific. In: Müller P, Henderson D (eds) Dynamics of oceanic internal gravity waves. 'Aha Huliko'a Hawaiian Winter Workshop, Hawaii Inst. Geophys. Spec. Publ. pp 205–213

Ingham MC (1966) The salinity extrema of the World Ocean. Dissertation, Oregon State University

Jenkins WJ (1982) Oxygen utilisation rates in the North Atlantic subtropical gyre and primary production in oligotrophic systems. Nature 300: 246–248

Karl DM, Letelier R, Hebel DV, Bird DF, Winn CD (1992) Trichodesmium blooms and new nitrogen in the North Pacific Gyre. In: Carpenter EJ, Capone D, Rueter JG (eds) Marine pelagic cyanobacteria: *Trichodesmium* and other diazotrophs. Kluwer Academic Boston pp 219–237

Kunze E (1987) Limits on growing finite length salt fingers: a Richardson number constraint. J Mar Res 45: 533–556

Laurent LS, Schmitt RW (1999) The contribution of salt fingers to vertical mixing in the North Atlantic tracer release experiment. J Physic Oceanogr 29: 1404–1424

Ledwell JR, Watson AJ, Law CS (1998) Mixing of a tracer in the pycnocline. J Geophys Res 103(C10): 21499–21529

Levitus S, Boyer TP (1994) World ocean atlas 1994, vol 4. Temperature. Noaa atlas nesdis 4, NOAA, Washington DC

Levitus S, Burgett R, Boyer TP (1994) World ocean atlas 1994, vol 3. Salinity. Noaa atlas nesdis 3, NOAA, Washington DC

Lewis MR, Harrison G, Oakey NS, Herbert D, Platt T (1986) Vertical nitrate fluxes in the oligotrophic ocean. Science 234: 870–873

Marmorino GO (1990) "Turbulent mixing" in a salt-finger staircase. J Geophys Res 95: 12983–12994

McClain CR, Firestone J (1993) An investigation of Ekman upwelling in the North Atlantic. J Geophys Res 98(C7): 12327–12339

McDougall TJ (1987) Thermobaricity cabbeling and water-mass conversion. J Geophys Res 92: 5448–5464

McDougall TJ (1991) Water mass analysis with three conservative variables. J Geophys Res 96(C5): 8687–8693

McDougall TJ, Ruddick BR (1992) The use of ocean microstructure to quantify both turbulent mixing and salt-fingering. Deep-Sea Res 39: 1931–1952

Minster JF, Boulahdid M (1987) Redfield ratios along isopycnal surfaces – a complementary study. Deep-Sea Res 34: 1981–2003

Osborn TR (1980) Estimates of the local rate of vertical diffusion from dissipation measurements. J Phys Oceanogr 10: 83–89

Oschlies A (2001) NAO-induced long-term changes in nutrient supply to the surface waters of the North Atlantic. Geophys Res Lett 28: 1751–1754

Oschlies A (2002a) Can eddies make ocean deserts bloom? Global Biogeoch Cycles 16: (4) p 1106, doi:10.1029/2001GB001830

Oschlies A (2002b) Nutrient supply to the surface waters of the North Atlantic: a model study. J Geophys Res 107(C5): p 3046, doi:10.1029/2000JC000275

Polzin K, Kunze E, Hummon J, Firing E (2002) The fine-scale response of lowered ADCP velocity profiles. J Atmosph Oceanic Technol 19: 205–224

Schmitt RW (1981) Form of the temperature-salinity relationship in the Central Water: evidence for double-diffusive mixing. J Phys Oceanogr 11: 1015–1026

Stommel H, Schott F (1977) The Beta Spiral and the determination of the absolute velocity field from hydrographic station data. Deep-Sea Res 24: 325–329

Turner JS (1965) The coupled turbulent transports of salt and heat across a sharp density interface. Int J Heat and Mass Trans 8: 759–767

Turner JS (1967) Salt fingers across a density interface. Deep-Sea Res 14: 599–611

Wijesekera H, Padman L, Dillon T, Levine M, Paulson C (1993) The application of internal-wave dissipation models to a region of strong mixing. J Phys Oceanogr 23: 269–286

Zhang J, Schmitt RW, Huang RX (1998) Sensitivity of the GFDL Modular Ocean Model to parameterization of double-diffusive processes. J Phys Oceanogr 28: 589–605

Salt-finger driven enhancement of upper ocean nutrient supply

A. Oschlies, H. Dietze and P. Kähler, 2003
Published in Geophysical Research Letters

GEOPHYSICAL RESEARCH LETTERS, VOL. 30, NO. 23, 2204, doi:10.1029/2003GL018552, 2003

Salt-finger driven enhancement of upper ocean nutrient supply

A. Oschlies, H. Dietze, and P. Kähler

Institut für Meereskunde and der Universität Kiel, Germany

Received 4 September 2003; accepted 21 October 2003; published 6 December 2003.

[1] In the subtropics, estimates of upper-ocean nitrate supply by turbulent mixing have been found insufficent to balance estimated nutrient loss through organic-matter export. Most mixing-rate estimates as well as numerical turbulence closure schemes commonly employed in numerical models have, however, neglected salt-finger induced mixing. Here we examine the potential contribution of salt-finger induced mixing to nutrient fluxes. Our model results suggest that salt-fingering instabilities generate substantial nutrient fluxes (on average 0.03 mol N m^{-2} yr^{-1}) which are of similar magnitude as fluxes associated with mechanically induced turbulence or with mesoscale eddies. Because salt-fingering activity depends on the proportion of temperature versus salinity effects on stratification rather than on the stability of stratification itself, its sensitivity to climate change will differ from that of "ordinary" mixing processes and needs to be considered in the context of global change. *INDEX TERMS:* 4805 Oceanography: Biological and Chemical: Biogeochemical cycles (1615); 4842 Oceanography: Biological and Chemical: Modeling; 4845 Oceanography: Biological and Chemical: Nutrients and nutrient cycling; 4568 Oceanography: Physical: Turbulence, diffusion, and mixing processes; 1635 Global Change: Oceans (4203). **Citation:** Oschlies, A., H. Dietze, and P. Kähler, Salt-finger driven enhancement of upper ocean nutrient supply, *Geophys. Res. Lett.*, *30*(23), 2204, doi:10.1029/2003GL018552, 2003.

1. Introduction

[2] Over much of the subtropical oceans, the surface heat flux is directed into the ocean and evaporation exceeds precipitation. As a result, warm and salty surface waters form, which overlie colder and fresher water. This can give rise to salt-fingering instabilities: Because on molecular scales, heat diffuses more rapidly than salt, downward moving warm and salty blobs exchange heat faster than salt and become denser, which reinforces their initial downward motion. Upward moving cold and fresh blobs warm and become lighter, which reinforces their upward motion. The blobs can thus extend vertically and form interleaving fingers which transport salt, and also nutrients with molecular diffusivities similar to that of salt, more efficiently than heat. The net effect of salt fingers can be described by macroscopic mixing with larger mixing rates for salt and nutrients than for heat [*Schmitt*, 2003] (i.e., a relation opposite to that of the molecular diffusivities which are larger for heat). Whenever salt-fingering instabilities occur, this adds to turbulent mixing brought about by shear instabilities, wind stirring, or buoyancy fluxes. It is these latter "ordinary" mixing processes which are usually considered for estimates of nutrient supply to date.

[3] Observational evidence for salt fingering has, among other regions, been reported for the upper Central Water of the subtropical thermocline [*Schmitt*, 1981]. The necessary condition for its occurence can be described quantitatively in terms of the density ratio $R_\rho = (\alpha T_z)/(\beta S_z)$, where α and β are the thermal expansion and haline contraction coefficients, and T_z and S_z are the vertical derivatives of the temperature and salinity fields, respectively [*Washburn and Käse*, 1987]. For $1 < R_\rho < 100$ the salt-fingering instability is theoretically permitted, but in an ocean constantly perturbed by internal-inertial motions substantial growth of the instabilities does usually not occur for R_ρ much larger than 2 [*Schmitt*, 1979]. Figure 1a shows the average distribution of R_ρ at the base of the euphotic zone (here chosen as z = 126 m) of the North Atlantic as derived from monthly climatological temperature and salinity fields [*Levitus and Boyer*, 1994; *Levitus et al.*, 1994], which for this depth level predict low values of R_ρ and hence a strong preference for salt fingering in the eastern part of the subtropics. In the following, a numerical ecosystem-circulation model is employed to examine the significance of salt fingering for the nutrient supply to the euphotic zone.

2. Model

[4] A simple nitrogen-based four-compartment ecosystem model [*Oschlies and Garçon*, 1999] is coupled to a circulation model which covers the North Atlantic between 15°S and 65°N at a resolution of 1/3 times 2/5 degrees in meridional and zonal direction, respectively. The model is forced by monthly mean wind stress and heat flux fields derived from the years 1989 to 1993 of the reanalysis project carried out at the European Centre for Medium-Range Weather Forecasts (ECMWF) [*Gibson et al.*, 1997]. The formulation of the non-solar part of the surface heat flux follows *Haney* [1971] with a flux-correction term that accounts for a heat-flux feedback from simulated surface temperature anomalies [*Barnier et al.*, 1995]. Because precipitation fields were considered to be not yet reliable enough, freshwater fluxes were parameterized by restoring surface salinity to observed monthly means taken from the *Levitus et al.* [1994] atlas. While in previous experiments vertical mixing was parameterized as "ordinary" turbulent mixing using the closure scheme of *Gaspar et al.* [1990], the present model version additionally includes salt-finger induced mixing. Its parameterisation proposed by *Zhang et al.* [1998] is in

0094-8276/03/2003GL018552$05.00

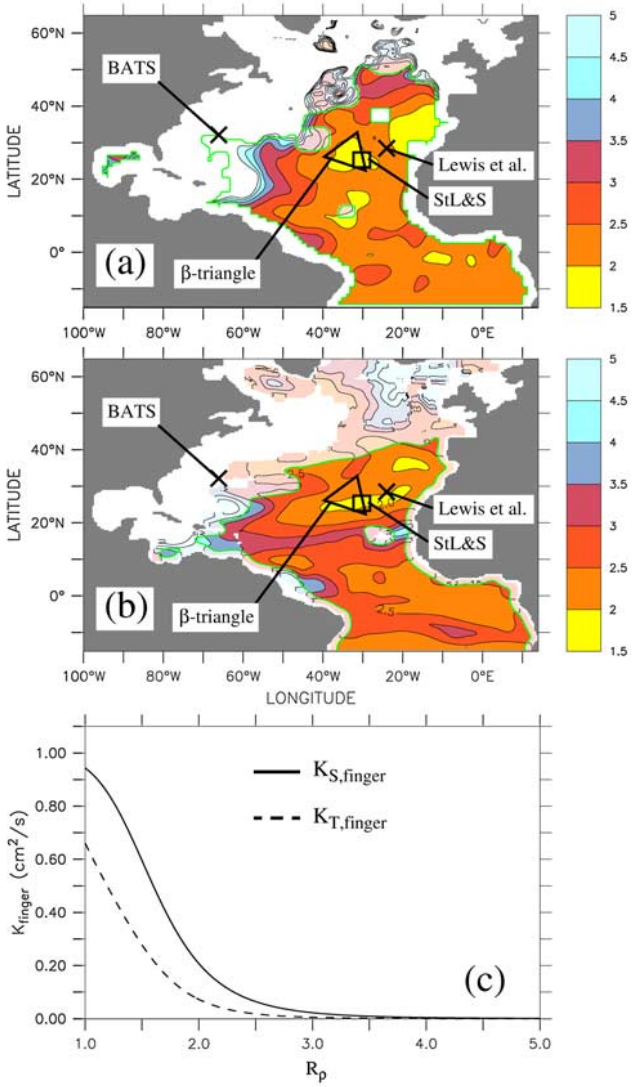

Figure 1. Density ratio $R_\rho = (\alpha T_z)/(\beta S_z)$ at the base of the euphotic zone (z = 126 m). Annual mean of R_ρ values computed (a) from monthly climatological temperature [*Levitus and Boyer*, 1994] and salinity [*Levitus et al.*, 1994] fields and (b) simulated by the ocean circulation model, whenever warm and salty water overlies colder and fresher water (i.e., $R_\rho > 1$). The area in which this criterion is satisfied all year round is enclosed by the green contour and displays the more intense colouring. (c) Salt-finger associated effective diffusivities for salt and nutrients, $K_{S,finger}$, and temperature, $K_{T,finger}$, according to the salt-fingering parameterisation of *Zhang et al.* [1998] employed in the circulation model. For $R_\rho > 1$, lowest R_ρ values are associated with largest salt-finger induced diffusivities. Because the relation is non-linear, average salt-finger induced diffusivities cannot be computed from average R_ρ values.

agreement with results from an elaborate analysis of microstructure measurements in the subtropical North Atlantic [*St. Laurent and Schmitt*, 1999] and was also found to perform well when applied to standard hydrographic measurements [*Dietze et al.*, 2003]. For R_ρ = 2, salt-finger associated diffusivities for salt and nutrients, $K_{S,finger}$, are about 0.2 cm^2 s^{-1} and increase to almost 1 cm^2 s^{-1} when R_ρ approaches unity (Figure 1c). For reference, mixing coefficients accounting for "ordinary" turbulent mixing are about 0.1 cm^2 s^{-1} in the stratified thermocline [*Ledwell et al.*, 1993; *St. Laurent and Schmitt*, 1999; *Polzin et al.*, 1995].

3. Results

[5] Simulated density ratios R_ρ reached after a 25-year spin-up period turn out to be in relatively good agreement with those observed (Figure 1) and also indicate the strong preference for salt fingering to occur at the base of the euphotic zone in the eastern part of the subtropical North Atlantic. The depth of lowest R_ρ values increases west-southwestward from about 120 m near 25°W to more than 300 m near the Caribbean Islands where observations have also confirmed intense salt-fingering activity [*Schmitt et al.*, 1987]. In the eastern part of the subtropical North Atlantic, both model results and monthly climatological data reveal a pronounced seasonal cycle of R_ρ values at depth levels down to about 200 m: R_ρ values reach minimum values of about 1.3 with associated salt-finger diffusivities of about 0.8 cm^2 s^{-1} in winter and spring during and after the warm and salty mixed layer has reached its maximum depth. Mixed layer deepening supplies salt from the evaporative surface layer to the pycnocline. On mixed-layer shoaling during spring, immediate salt supply from the sea surface ceases and density ratios increase above 1.6 and salt-finger induced mixing rates become smaller than 0.5 cm^2 s^{-1} within a period of about two months. A comparison of simulated salt-finger induced diffusivities with observational estimates shows particularly good agreement (within 15%) when the time interval of model output and observations is the same (Table 1). Adding the salt-fingering parameterisation was found to result in a very small decrease of sea surface temperatures (on average by 0.01°C) and salinities (by 0.004 psu) with associated changes in simulated heat input (0.5 W m^{-2}) and evaporation minus precipitation (0.03 m yr^{-1}).

[6] Annual nitrate supply simulated by the coupled ecosystem-circulation model including the salt-fingering parameterisation of *Zhang et al.* [1998] is shown in Figure 2a. Over large parts of the subtropical North Atlantic the model suggests a two- to fivefold higher nutrient supply compared to the case without salt-finger induced mixing. At the individual subtropical sites marked in Figure 2, salt fingering accounts for up to 80% of the total nitrate supply (Table 1). Such values are within the bounds of an earlier re-assessment of microstructure data suggesting that observational estimates of diffusive nitrate supply be revised upward by up to a factor of six if salt fingering were the dominant mixing mechanism [*Hamilton et al.*, 1989]. Averaged over the eastern part of the oligotrophic subtropical gyre (45–20°W, 20–30°N), salt-finger induced nitrate supply in our model amounts to 0.03 mol m^{-2} yr^{-1} (Figure 2b) and approximately doubles previous estimates of diffusive supply that did not take salt fingering into account [*Oschlies*, 2002a]. It is noteworthy that for this region the simulated nutrient supply by salt fingering is of similar size as that by

Table 1. Salt-finger Induced Diffusivities and Nitrate Supply at z = 126 m

	Lewis et al. (23W, 28.5N)	StL&S (31–26.8W, 24–25.7N)	β triangle, 30W (30W, 24–31.5N)	BATS (65W, 32.5N)
		Salt-finger induced tracer diffusivities ($cm^2 s^{-1}$)		
$K_{S,finger}$(obs, $\overline{month}$)	0.22[a]	0.46[b]	0.58[c]	
$K_{S,finger}$(mod, $\overline{month}$)[d]	0.19[a]	0.40[b]	0.53[c]	
$K_{S,finger}$(mod, $\overline{yr}$)	0.23	0.28	0.26	0.04
		Nitrate fluxes (mol N $m^{-2} yr^{-1}$)		
salt finger contr.[e]	0.042	0.053	0.052	0.082
total supply	0.062	0.065	0.067	0.465

[a]June, observational estimate from *Hamilton et al.* [1989].
[b]April, observational estimate from *St. Laurent and Schmitt* [1999].
[c]March, observational estimate from *Dietze et al.* [2003].
[d]Model estimates of $K_{S,finger}$ ($\overline{month}$) are consistently lower than the observational estimates by some 10%, indicating that our estimate of salt-finger induced nitrate supply may be slightly too low.
[e]Difference between simulations with and without salt-fingering parameterisation (i.e., includes non-linear effects due to changes in density field and circulation).

mesoscale eddies which, so far, have received considerably more attention. [*McGillicuddy et al.*, 1998; *Oschlies and Garçon*, 1998; *Oschlies*, 2002b].

4. Discussion

[7] Despite its substantial contribution to the upper-ocean nutrient supply in the North Atlantic subtropical gyre, salt fingering alone does not seem to be sufficient to close the gap between previous estimates of nitrate supply [*Lewis et al.*, 1986] and export of organic matter in the eastern part of the subtropical North Atlantic [*Jenkins*, 1982]. Recent observations near 30°W show, however, that the apparent observational discrepancy can be reconciled when, in addition to salt-finger induced mixing, nitrogen fixation and the export of carbon-rich organic matter are considered [*Kähler et al.*, High rates of nitrogen fixation and TOC subduction in the eastern subtropical North Atlantic, submitted manuscript.

[8] An interesting aspect of salt-finger induced mixing is its strong dependence on water mass properties as expressed in the density ratio, i.e., in the relative contributions of temperature and salinity to the vertical density gradient. When these water mass properties change in response to changing atmospheric forcing, salt-finger induced mixing will be affected in a different way than "ordinary" turbulent mixing which seems to be relatively insensitive to changes in water column properties [*Polzin et al.*, 1995]. Present climate models, which do not take into account salt-finger induced mixing, tend to predict largest changes in mixing and nutrient supply over the next century to occur at high latitudes [*Sarmiento et al.*, 1998]. However, temperature- and precipitation/evaporation-driven changes in the density ratios simulated by such models suggest substantial impacts on salt-fingering activity in low-latitude surface waters. For example, the Geophysical Fluid Dynamics Laboratory (GFDL) coupled climate model [*Delworth et al.*, 2002] predicts a more than 30% decrease of the area with density ratios in the range $1 < R_\rho < 2$ at the base of the euphotic zone in the subtropical and tropical North Atlantic within this century. Such estimates are still uncertain, particularly as they are very sensitive to prognosed changes in precipitation patterns. Nevertheless, the peculiar, and so far in this context neglected, feature of different molecular diffu-

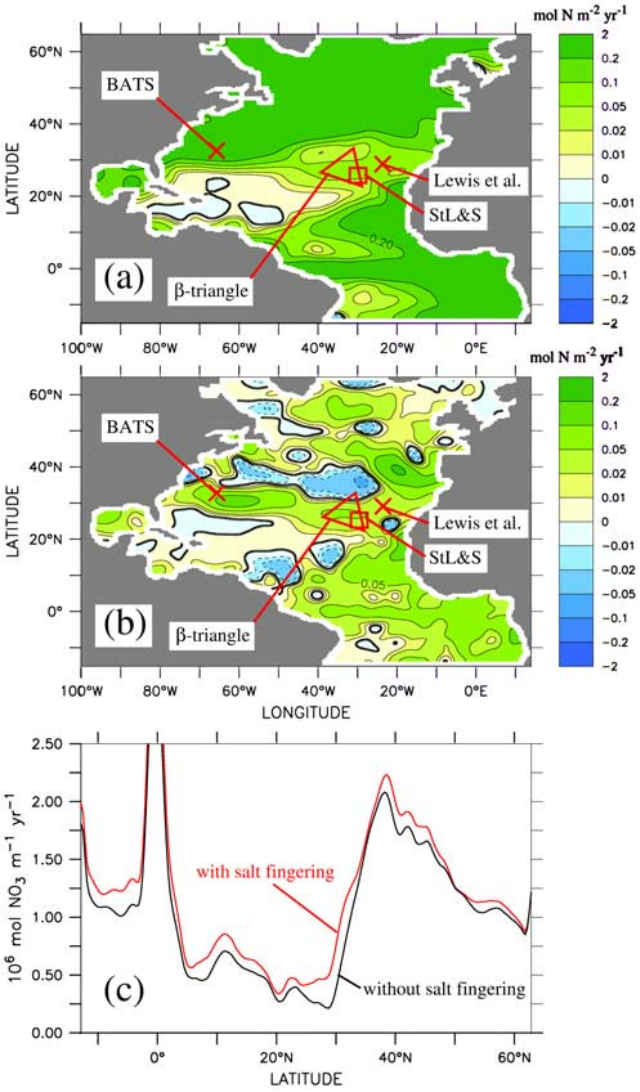

Figure 2. (a) Nitrate supply to the upper 126 m simulated by the experiment with salt-fingering parameterisation included. (b) Nitrate supply simulated by the experiment with salt-fingering parameterisation minus nitrate supply simulated by the experiment without this parameterisation. (c) Zonally integrated nitrate supply simulated by the experiment with (red line) and without (black line) salt fingering.

sivities for temperature and salt will certainly contribute to anticipated large-scale changes in marine biological production.

[9] **Acknowledgments.** We acknowledge funding by the Deutsche Forschungsgemeinschaft and thank one anonymous reviewer for helpful and constructive comments.

References

Barnier, B., L. Siefridt, and P. Marchesiello, Surface thermal boundary condition for a global ocean circulation model from a three-year climatology of ECMWF analyses, *J. Mar. Syst.*, *6*, 363–380, 1995.

Delworth, T. L., et al., Review of simulations of climate variability and change with the GFDL R30 coupled climate model, *Climate Dyn.*, *19*, 555–574, 2002.

Dietze, H., A. Oschlies, and P. Kähler, Internal-wave induced and double-diffusive nutrient fluxes to the nutrient-consuming surface layer in the oligotrophic subtropical North Atlantic, *Ocean Dynamics*, in press, 2003.

Gaspar, P., Y. Gregoris, and J.-M. Lefevre, A simple eddy kinetic energy model for simulations of the oceanic vertical mixing: Tests at station Papa and Long-Term Upper Ocean Study site, *J. Geophys. Res.*, *95*, 16,179–16,193, 1990.

Gibson, J. K., et al., *ECMWF Re-Analysis Project Report Series. 1. ERA Description*, 72 pp., European Centre for Medium-Range Weather Forecasting, Reading, UK, 1997.

Hamilton, J. M., M. R. Lewis, and B. R. Ruddick, Vertical fluxes of nitrate associated with salt fingers in the World's Oceans, *J. Geophys. Res.*, *94*, 2137–2145, 1989.

Haney, R. L., Surface thermal boundary condition for ocean circulation models, *J. Phys. Oceanogr.*, *1*, 241–248, 1971.

Jenkins, W. J., Oxygen utilization rates in North Atlantic subtropical gyre and primary production in oligotrophic systems, *Nature*, *300*, 246–248, 1982.

Ledwell, J. R., A. J. Watson, and C. S. Law, Evidence for slow mixing across the pycnocline from an open-ocean tracer-release experiment, *Nature*, *364*, 701–703, 1993.

Levitus, S., and T. Boyer, World Ocean Atlas 1994, Vol. 4: Temperature. *NOAA Atlas NESDIS 4*, U.S. Gov. Print. Office, Washington, D.C., 99 pp., 1994.

Levitus, S., R. Burgett, and T. P. Boyer, World Ocean Atlas 1994, Vol. 3: Salinity. *NOAA Atlas NESDIS 3*, U.S. Gov. Print. Office, Washington, D.C., 99 pp., 1994.

Lewis, M. R., W. G. Harrison, N. S. Oakey, D. Herbert, and T. Platt, Vertical nitrate fluxes in the oligotrophic ocean, *Science*, *234*, 870–873, 1986.

McGillicuddy, D. J., Jr., et al., Influence of mesoscale eddies on new production in the Sargasso Sea, *Nature*, *394*, 263–266, 1998.

Oschlies, A., Nutrient supply to the surface waters of the North Atlantic: A model study, *J. Geophys. Res.*, *107*(C5), doi:10.1029/2000JC000275, 2002a.

Oschlies, A., Can eddies make ocean deserts bloom?, *Global Biogeochem. Cycles*, *16*, 1106, doi:10.1029/2001GB001830, 2002b.

Oschlies, A., and V. Garçon, Eddy-induced enhancement of primary production in a model of the North Atlantic Ocean, *Nature*, *394*, 266–269, 1998.

Oschlies, A., and V. Garçon, An eddy-permitting coupled physical-biological model of the North Atlantic. Part I: Sensitivity to advection numerics and mixed layer physics, *Global Biogeochem. Cycles*, *13*, 135–160, 1999.

Polzin, K. L., J. M. Toole, and R. W. Schmitt, Finescale parameterizations of turbulent dissipation, *J. Phys. Oceanogr.*, *25*, 306–328, 1995.

Sarmiento, J. L., T. M. C. Hughes, R. J. Stouffer, and S. Manabe, Simulated response of the ocean carbon cycle to anthropogenic climate warming, *Nature*, *393*, 245–249, 1998.

Schmitt, R. W., The growth rate of super-critical salt fingers, *Deep-Sea Res.*, *26*, 2589–2605, 1979.

Schmitt, R. W., Form of the temperature-salinity relationship in the Central Water: Evidence for double-diffusive mixing, *J. Phys. Oceanogr.*, *11*, 1015–1026, 1981.

Schmitt, R. W., Observational and laboratory insights into salt finger convection, *Progr. Oceanogr.*, *56*, 419–433, 2003.

Schmitt, R. W., H. Perkins, J. D. Boyd, and M. C. Stalcup, C-SALT: An investigation of the thermohaline staircase in the western tropical North Atlantic, *Deep-Sea Res.*, *34*, 1655–1665, 1987.

St. Laurent, L., and R. W. Schmitt, The contribution of salt fingers to vertical mixing in the North Atlantic tracer release experiment, *J. Phys. Oceanogr.*, *29*, 1404–1424, 1999.

Washburn, L., and R. H. Käse, Double diffusion and the distribution of the density ratio in the Mediterranean waterfront southeast of the Azores, *J. Phys. Oceanogr.*, *17*, 12–25, 1987.

Zhang, J., R. W. Schmitt, and R. X. Huang, Sensitivity of the GFDL Modular Ocean Model to parameterization of double-diffusive processes, *J. Phys. Oceanogr.*, *28*, 589–605, 1998.

A. Oschlies, H. Dietze, and P. Kähler, Institut für Meereskunde, Düsternbrooker Weg 20, 24105 Kiel, Germany. (aoschlies@ifm.uni-kiel.de; hdietze@ifm.uni-kiel.de; pkaehler@ifm.uni-kiel.de)

Modeling abiotic production of apparent oxygen utilisation in the oligotrophic subtropical North Atlantic

H. Dietze and A. Oschlies, 2004
Submitted to Ocean Dynamics

Ocen Dynamics manuscript No.
(will be inserted by the editor)

Modeling abiotic production of apparent oxygen utilisation in the oligotrophic subtropical North Atlantic

Heiner Dietze, Andreas Oschlies

Institut fuer Meereskunde, Kiel, e-mail: hdietze@ifm.uni-kiel.de

Received: date / Revised version: date

Abstract Apparent oxygen utilisation is potentially biased by abiotic, physical processes. Using a coupled 3-D circulation-oxygen model this potential is quantitatively estimated for a region in the eastern subtropical North Atlantic, called the Beta Triangle.
There, an inconsistency exists between estimates of high carbon export from the euphotic zone, based on oxygen utilisation rates in the thermocline (JENKINS (1987)), and those of low nutrient supply to the euphotic zone (LEWIS ET AL. (1986), DIETZE ET AL. (2004)).
Results indicate that the JENKINS (1987) estimate is indeed biased high by O(10%) due to abiotic processes feigning respiration on respective isopycnals. Vertical integration, however, yields an abiotic fraction of less than 3%, so the apparent observational discrepancy can not be resolved.

1 Introduction

Apparent oxygen utilisation (AOU) of seawater is defined as the amount of diluted oxygen missing to a 100% saturation. Generally it is assumed that this deficit is caused by biology i.e. net respiration although a fraction of it might be produced or hidden by abiotic processes. These abiotic processes are: 1. subduction of under- or oversaturated water, 2. mixing of water-parcels with different salinities and temperatures as the saturation of oxygen in seawater is a nonlinear function of these properties, 3. double diffusion and convective layering resulting in different vertical diffusivities for oxygen and heat, 4. solar heating of water-parcels which are not in contact with the atmosphere.
There is evidence that these processes significantly alter biotically inferred AOU: RUSSELL AND DICKSON (2003) showed that South Pacific Antarctic Intermediate Water is subducted with an oxygen saturation of less than 85%. They argue that this can not be explained by biotic activity as solar radiation and temperatures are very low in the region of subduction. Another example from the eastern subtropical North Atlantic (Fig. 1, Station S) based on measurements of argon and oxygen within the euphotic zone was reported by SPITZER AND JENKINS (1989). They showed that abiotically effected oxygen oversaturation exceeds 4% in summer.
This study aims to quantify uncertainties due to abiotic processes imposed on oxygen utilisation rates (OUR) in the eastern subtropical North Atlantic as estimated by JENKINS (1982).
JENKINS (1982) measured AOU, tritium, and ^{3}He on isopycnals within the so-called Beta Triangle (Fig. 1, named after the beta-spiral method applied to hydrographic section data (STOMMEL AND SCHOTT (1977))). Least-square linear regression between AOU and age, derived from the transient tracer pair, yielded OUR. Vertical integration corresponded to an average export of organic matter from the surface ocean of $47\,\mathrm{gCm^{-2}a^{-1}}$. This result is not consistent with estimates of new production, which in steady state should equal export production (EPPLEY AND PETERSON (1979)). New production, derived from nitrate supply to the surface layer

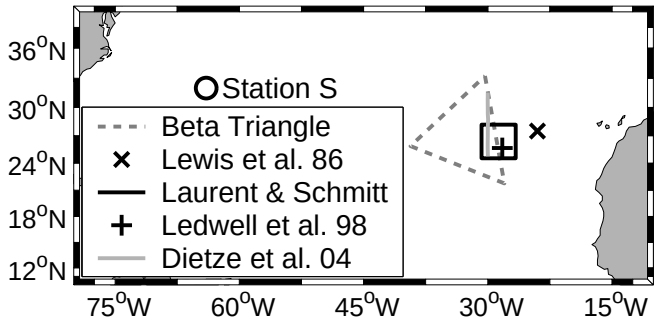

Fig. 1 Locations of this and related studies.

* We acknowledge discussions with Carsten Eden and funding by the Deutsche Forschungsgemeinschaft.

(LEWIS ET AL. (1986), DIETZE ET AL. (2004)) amounts to only less than 20% of the export estimate of JENKINS (1982).
There are several potential explanations for this apparent discrepancy that can be thought of. Explanations focussing on biogeochemical processes include: 1. different scales of time and space in the two respective studies, 2. nitrogen sources other than nitrate (N_2-fixation, dissolved organic nitrogen, atmospheric deposition), 3. export of carbon-rich organic matter (e.g. dissolved organic carbon), 4. vertically migrating organisms influencing the nutrient and oxygen distributions. The present model study does not adress these biogeochemical issues but instead examines the potential of abiotically produced AOU to resolve the apparent discrepancy between measured OUR and nitrate supply to the surface layer of the study area.

2 Method

An oxygen compartment, treated like an inert gas (e.g. argon), is embedded into a $2/5° \times 1/3°$ resolution circulation model of the North Atlantic with a turbulence closure scheme adequate to simulate the seasonal mixed-layer cycle and diffusion in the main thermocline (OSCHLIES ET AL. (2000)). An additional parameterization for double diffusive fluxes according to ZHANG ET AL. (1998) ensures vertical diffusivities consistent with observations within the main thermocline of the North Atlantic subtropical gyre (OSCHLIES ET AL. (2003)).
Numerical advection and diffusion schemes used in this model study were shown by EDEN AND OSCHLIES (2003 subm.) to reproduce results of the LEDWELL ET AL. (1998) tracer release experiment.
The atmospheric forcing consists of monthly mean wind stress and heat flux fields derived from the years 1989-1993 of the reanalysis project carried out at the European Centre for Medium-Range Weather Forecasts (ECMWF) (GIBSON ET AL. (1997)). Freshwater fluxes are parameterized by restoring surface salinity to observed monthly means taken from the LEVITUS ET AL. (1994) atlas. The formulation of the surface heat flux follows HANEY (1971). Solar heat flux penetrates into the ocean. Absorbtion is parameterized using the water type I of JERLOV (1976) unless stated differently.
All simulations were integrated for 23 years starting from a common spun-up state of the circulation model and oxygen concentrations corresponding to 100% saturation. Oxygen is continuously, i.e. every timestep, reset to 100% saturation at the restoring zones of the circulation model (Mediterranean outflow, northern and southern boundary of the model domain i.e. 15°S and 65°N).
Air-to-sea oxygen flux FO_2 is modeled following the OCMIP-2 (R. G. Najjar and J. C. Orr, Design of OCMIP-2 simulations of chlorofluorocarbons, the solubility pump and common biogeochemistry, 1998; available from the World Wide Web at http://www.ipsl.jussieu.fr/OCMIP) guideline:

$$FO_2 = KW \left(O_2^{sat} - O_2^{surf} \right) \tag{1}$$

where O_2^{sat} is the oxygen concentration corresponding to a 100% saturation according to GARCIA AND GORDON (1992), O_2^{surf} is oxygen concentration in the uppermost grid box and KW is the piston velocity, calculated according to:

$$KW = a\,(u2 + v)\,(ScO_2/660)^{-1/2} \tag{2}$$

whith coefficient $a = 0.337/3.610^5$s/m and the Schmidt number of oxygen in seawater ScO_2 as a function of temperature as proposed by KEELING ET AL. (1998). The square of monthly mean windspeed $u2$ and the variance v of windspeed computed over one month were calculated from ECMWF climatology (using the same database which drives the circulation model). A crude ice model switches off air-to-sea oxygen fluxes whenever sea-surface temperatures drop below -1.8°C.
Furthermore a primitive age tracer was integrated for 23 years by counting up time in every grid box, except at the surface where age was continuously reset to zero.
Following JENKINS (1982), rates of abiotically induced AOU are calculated by least-square linear regression between modeled abiotically effected AOU and model age on isopycnals.
Note that in this study AOU refers to deviations from saturation effected by physical processes rather than by net biotic respiration.

3 Abiotic oxygen utilisation rates in the Beta Triangle region

Modeled abiotic oxygen along 30°W within the Beta Triangle shows significant deviations from a 100% saturation (Fig. 2) in October. The strongest deviation from saturation is below the mixed layer where oversaturation reaches values up to 6 mmol O_2/m^3 corresponding to 3.6%. This oversaturation decays during mixed-layer deepening in autumn and winter and builds up between spring and autumn. Its magnitude can be explained by solar radiation penetrating below the mixed layer: This heat flux warms water which is not in contact with the atmosphere. As the water warms the oxygen concentration corresponding to a 100% saturation decreases while the concentration of oxygen molecules stays constant. Hence, in this case, heat fluxes can be translated into AOU fluxes $FAOU_{sol}$:

$$FAOU_{sol}\,(z) = -\frac{\partial O_2^{sat}}{\partial T} \frac{Q(z)_{sol}}{C_p} \tag{3}$$

where $Q(z)$ is solar heat flux at depth z, C_p is the specific heat of seawater and O_2^{sat} is oxygen concentration

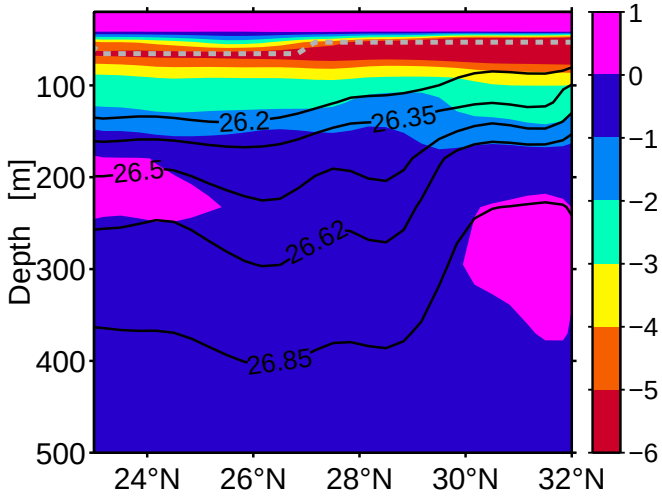

Fig. 2 Meridional section of modeled abiotically effected AOU (filled contours) and σ_0 (labeled contours) along 30°W within the Beta Triangle in October. Units are mmol O_2/m^3, negative values denote oversaturation. Grey line is mixed-layer depth, here defined as the depth where density σ_0 is 0.125 higher than the density at the surface.

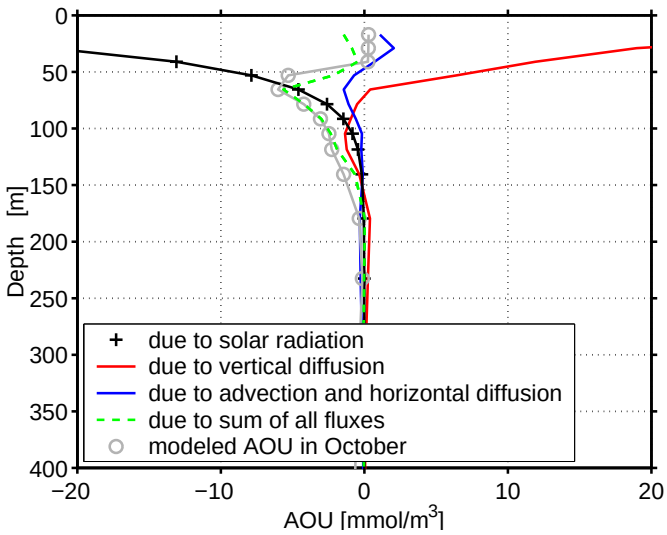

Fig. 3 Mean of the integral of abiotically induced AOU fluxes due to respective mechanisms from March till October within the Beta Triangle. The water column is almost saturated in March, so that the integral of all AOU fluxes from March till October essentially coincides with modeled AOU found October.

corresponding to a 100% saturation according to Garcia and Gordon (1992). Integration of $FAOU_{sol}$ from March till October yields AOU high enough to explain the modeled AOU maximum in October (Fig. 3).
An analog formulation to equation (3) yields AOU fluxes $FAOU_{mech}$ due to respective transport mechanisms mech:

$$FAOU_{mech} = \frac{\partial O_2^{sat}}{\partial T}\frac{Q_{mech}}{C_p} + \frac{\partial O_2^{sat}}{\partial S} FS_{mech} - FO_{mech} \tag{4}$$

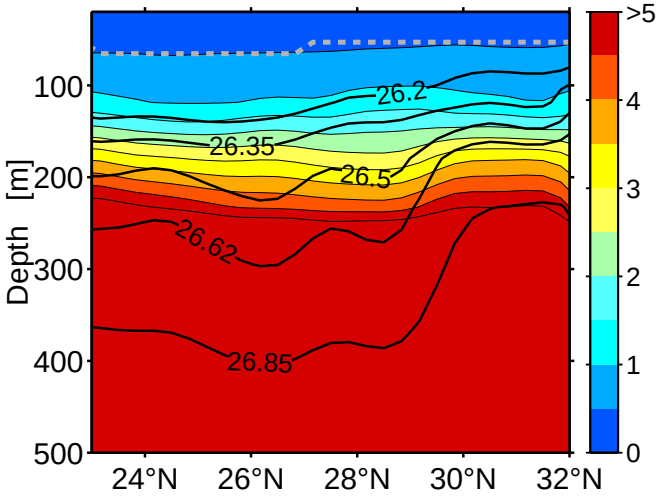

Fig. 4 Meridional section of modeled age (filled contours) and σ_0 (labeled contours) along 30°W within the Beta Triangle in October. The unit of age is years. The dashed line refers to mixed-layer depth, here defined as the depth where density σ_0 is 0.125 higher than the density at the surface.

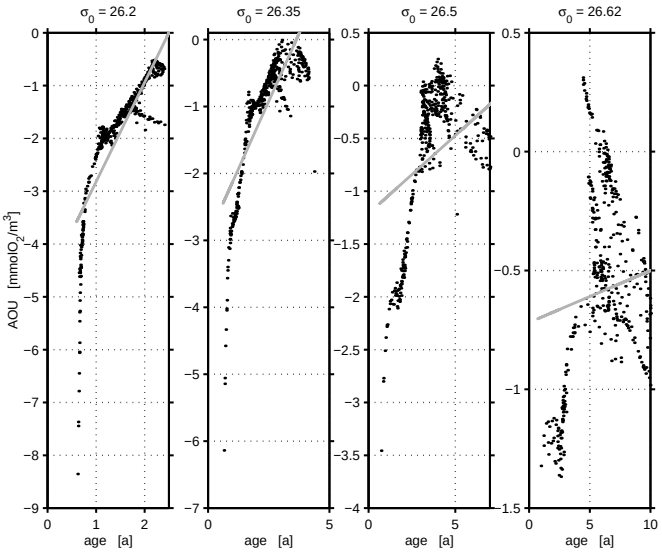

Fig. 5 Modeled abiotically effected AOU found within the Beta Triangle on respective isopycnals in October plotted against modeled age. The grey lines denote least-square linear regressions. Their slopes are listed in Tab. 1.

where FS_{mech} is salt flux and FO_{mech} is oxygen flux due to respective mechanisms. Fig. 3 shows AOU fluxes due to vertical diffusion and due to the sum of of horizontal diffusion and advection integrated from March till October. The AOU distribution is governed by the balance between the oversaturating effect of solar radiation and vertical diffusive transport of oversaturated water into the mixed layer. All the other processes listed in the introduction are of minor importance although two of them leave their imprint on the AOU distribution shown in Fig. 2:
The slight undersaturation (i.e. positive AOU) within

the mixed layer is caused by an oceanic heat loss of $73\,W/m^2$ combined with finite air-sea gas exchange.
The distribution of AOU below the maximum of oversaturation is slightly influenced by salt-fingering as this is the only process capable of producing undersaturation in this depth. (A model run without double diffusion did not show any undersaturation in this region, so spurious numerical effects rule out as an explanation.) Note that ordinary mixing of two water parcels does always result in a mixed parcel oversaturated relative to the mean saturation of the original parcels. This behaviour is set by the nonlinear relationship between temperature, salinity and saturation.
Double diffusion, or salt fingering, is different as it results in effective diffusivities for molecules being higher than those for heat. Depending on gradients of temperature, salinity, and oxygen a waterparcel, heated by salt fingering can at the same time, and by the same process, loose oxygen so fast that undersaturation evolves.
Model age in October (Fig. 4) increases with depth. Following an isopycnal from the North to the South within the upper 200 m, it gets deeper, which means further away from the maximum of oversaturation, and older. Hence, a linear regression between modeled AOU and model age on isopycnals yields positive oxygen utilisation rates (Fig. 5) feigning biotic respiration.
Intercomparison with OUR measured by JENKINS (1982) (who measured the sum of biotically and abiotically inferred OUR in October) in the Beta Triangle (Tab. 1) shows that the abiotic fraction reaches values exceeding 12% on the uppermost isopycnal $\sigma_0 = 26.2$
JENKINS (1982) calculated net oxygen consumed in the water column by integrating a fitted (in least-square sense) log linear consumption rate-depth dependence between 100 m and infinity. Following his approach with modeled OUR yields an abiotic rate corresponding to 2.7% of the JENKINS (1982) estimate.

σ_0	Depth [m] J. 1987	OUR J. 1987	Depth [m] modeled	abiotic OUR modeled
26.20	111	15.6	129	1.88
26.35	138	14.4	161	0.81
26.5	191	8.9	211	0.15
26.62	258	9.6	264	0.02

Table 1 OUR on and depth of respective isopycnal estimated by JENKINS (1987) and modeled in this study. Unit of OUR is mmol $O_2/m^3/a$.

4 Discussion

The cruical question is, to what extend the modeled abiotic OURs are realistic. Thus abiotic AOU distribution and vertical alignment of age on respective isopycnals have to be validated.
The vertical alignment of age on an isopycnal is a consequence of direct Ekman pumping and the subduction of water due to southward shoaling of the winter mixed layer. One measure of the subduction rate is the velocity $w_s = 1/\frac{\delta\tau}{\delta z}$ derived from the mean vertical age gradient (JENKINS (1987)). Intercomparison between modeled w_s and estimates of JENKINS (1987) based on observations (Tab. 3) shows good agreement at least for the upper two isopycnals which contribute the lions part of abiotic OUR in the water column.

σ_0	w_s [m/a] JENKINS (1987)	w_s [m/a] modeled
26.20	40	46
26.35	44	36
26.5	39	26
26.62	79	22

Table 2 Observed and modeled subduction rates, derived from the mean of vertical age gradients in the Beta Triangle.

The modeled distribution of abiotic AOU in the region under consideration was shown to be determined by the interplay between vertical penetration of solar radiation and vertical diffusion. To what extend is that interplay realistically modeled? Intercomparison with measurements of dissolved argon can give an answer to that question since argon is an inert gas whose physical properties (e.g. solubility and diffusivity) are close to those of oxygen and have a similar temperature dependence (BENSON (1965)).
Unfortunately argon measurements are not that widespread. The best we can do here, is using the dataset of SPITZER AND JENKINS (1989) at Station S (32°N 64°W) near Bermuda. Fig. 6 shows time series of temperature and argon oversaturation measured during April 1985 - April 1986 as well as modeled temperature and abiotic oxygen oversaturation. We conclude that the model is capable of reproducing the mixed-layer depth and gets roughly the right amount of oversaturation in the seasonal thermocline.
Note that the model used in this study predicts the right amount of oversaturation without air injection at the surface via bubble entrainment, while SPITZER AND JENKINS (1989) conclude, based on a 1-D vertical bulk mixed layer model that 40% of the subsurface oversaturation in summer is due to bubble entrainment. Apart from the missing oversaturating effect of bubble entrainment (and the 3-D approach) the model used in this study has two substantial differences: 1. Jerlov water type I was used instead of IA, i.e. solar radiation penetrates deeper into the ocean. 2. Vertical diffusivities set by the turbulence closure scheme and the parameterization of double diffusion below the mixed layer are 80% lower than the $1 cm^2 s^{-1}$ prescribed by SPITZER AND

JENKINS (1989). These lower diffusivities coincide better with observational estimates of LEDWELL ET AL. (1998) and LAURENT AND SCHMITT (1999).
A model run with a Jerlov water type changed from I to IA reduced the maximum of oversaturation by only 0.1%. So the fundamental difference between the two models is that the SPITZER AND JENKINS (1989) model predicts a higher loss of oversaturation below the mixed layer due to upwards diffusive transport which is compensated by bubble entrainment from the surface.
The evaluation of the parameterization of bubble entrainment used by SPITZER AND JENKINS (1989) is beyond the scope of this work. Here, we just want to note that a suite of model runs with different surface boundary conditions for oxygen (halved piston velocity, prescribed saturation at the surface, prescibed oversaturation of 3% at the surface mimicking the oversaturating effect of bubble entrainment) showed that the abiotic OUR estimate ($154\,mmol\,O_2/m^2/a$) is relatively insensitive towards these changes (all model estimates are within 127 to $164\,mmol\,O_2/m^2/a$).
Another potential caveat is numerical dispersion: The model uses a central-difference advection scheme. These schemes are known to cause numerical dispersion (e.g. OSCHLIES (1999)) which is dependent on the respective tracer gradient. As oxygen and temperature gradients do not need to be identical, numerical dispersion may produce under- as well as oversaturation. In the region under consideration, however, these effects can be neglected as it was shown that the combined effect of advection and horizontal diffusion on AOU distribution is relatively small (Fig. 3).

5 Conclusion

The coupled 3-D circulation-oxygen model used in this study has proved to be successful in studying abiotically produced apparent oxygen utilisation in the subtropical gyre of the North Atlantic. Fundamental differences compared with an earlier 1-D approach (SPITZER AND JENKINS (1989)) were the neglect of air injection by bubble entrainment at the surface and lower vertical diffusivities being more consistent with observations.
Modeled subduction rates within the eastern subtropical gyre of the North Atlantic at a site called the Beta Triangle, were in good agreement with the observational estimates of JENKINS (1987). Thus it was possible to calculate the abiotic fraction of the oxygen utilisation rates estimated by JENKINS (1987):
On the uppermost isopycnal $\sigma_0 = 26.2$ used in the repective study the abiotic effect was found to exceed 10%. The vertical integral, however, showed a bias of less than 3%. So we can conclude that while abiotic oxygen utilisation was shown to considerably effect the South Pacific Antarctic Intermediate Water by RUSSELL AND DICKSON (2003) it is of minor importance in the subtropical North Atlantic.
Evidently other mechanisms than abiotically inferred oxygen utilisation rates need to be examined to reconcile the apparent discrepancy between nutrient supply and estimated organic-matter export derived from oxygen consumption.

References

BENSON, B. B., 1965: Some thoughts on gases dissolved in the oceans. In: *Proc. Symp. on Mar. Geochem*, D. R. Schink and J. T. Corless, Hg., Univ. of Rhode Island Occasional Publ., p. 91–107.

DIETZE, H., A. OSCHLIES and P. KÄHLER, 2004: Internal-wave induced and double-diffusive nutrient fluxes to the nutrient-consuming surfcae layer in the oligotrophic subtropical North Atlantic. *Ocean Dynamics*, **54** (1), p. doi:10.1007/s10236–003–0054–7.

EDEN, C. and A. OSCHLIES, 2003 subm.: Effective diffusivities in models of the North Atlantic. Part I: subtropical thermocline. *Journal of Physical Oceanography.*

EPPLEY, R. W. and B. J. PETERSON, 1979: Particulate organic matter flux and planktonic new production in the deep ocean. *Nature*, **282**, p. 677–680.

GARCIA, H. E. and L. I. GORDON, 1992: Oxygen solubility in seawater: better fitting equations. *Limnol. Oceanogr.*, **37(6)**, p. 1307–1312.

GIBSON, J. K., P. KALLBERG, S. UPPALA, A. HERNANDEZ, A. NOMURA and E. SERRANO, 1997: ECMWF Re-Analysis Project report series. *ERA description, Eur. Cent. for Medium-Range Weather Forecasting, Reading, UK*, **1**, p. 72pp.

HANEY, R. L., 1971: Surface thermal boundary conditions for ocean circulation models. *Journal of Physical Oceanography*, **1**, p. 241–248.

JENKINS, W. J., 1982: Oxygen utilisation rates in North Atlantic subtropical gyre and primary production in oligotrophic systems. *Nature*, **300**, p. 246–248.

JENKINS, W. J., 1987: 3H and 3He in the Beta Triangle: Observations of Gyre Ventilation and Oxygen Utilisation Rates. *Journal of Physical Oceanography*, **17**, p. 763–783.

JERLOV, N. G., 1976: Marine Optics. *Elsevier New York.*

KEELING, R. F., B. B. STEPHENS, R. G. NAJJAR, S. C. DONEY, D. ARCHER and M. HEIMANN, 1998: Seasonal variations in the atmospheric O2/N2 ratio in relation to the kinetics of air-sea gas exchange. *Global Biogeochemical Cycles*, **12**, p. 141–163.

LAURENT, L. S. and R. W. SCHMITT, 1999: The contribution of Salt Fingers to vertical mixing in the North Atlantic Tracer Release Experiment. *Journal of Physical Oceanography*, **29**, p. 1404–1424.

LEDWELL, J. R., A. J. WATSON and C. S. LAW, 1998: Mixing of a tracer in the pycnocline. *Journal of Geophysical Research*, **103 (C10)**, p. 21,499–21,529.

LEVITUS, S., R. BURGETT and T. P. BOYER, 1994: World Ocean Atlas 1994. Volume 3: Salinity. Noaa atlas nesdis 3, NOAA, Washington D.C.

LEWIS, M. R., G. HARRISON, N. S. OAKEY, D. HERBERT and T. PLATT, 1986: Vertical nitrate fluxes in the oligotrophic ocean. *Science*, **234**, p. 870–873.

OSCHLIES, A., 1999: An unrealistic high-salinity tongue simulated in the tropical Atlantic: another example illustrating the need for a more careful treatment of vertical discretizations in OGCMs. *Ocean Modeling*, **1**, p. 101–109.

OSCHLIES, A., H. DIETZE and P. KÄHLER, 2003: Salt-finger driven enhancement of upper ocean nutrient supply. *Geophysical Research Letters*, **30** (23), p. doi:10.1029/2003/GL018552.

OSCHLIES, A., W. KOEVE and V. GARÇON, 2000: An eddy-permitting coupled physical-biological model of the North Atlantic. Part II: Ecosystem dynamics and comparison with satellite and JGOFS local studies data. *Global Biogeochemical Cycles*, **14**, p. 499–523.

RUSSELL, J. L. and A. G. DICKSON, 2003: Variability in oxygen and nutrients in South Pacific Antarctic Intermediate Water. *Global Biogeochemical Cycles*, **17 (2)**, p. 1033, doi:10.1029/2000GB001317.

SPITZER, W. S. and W. J. JENKINS, 1989: Rates of vertical mixing, gas exchange and new production: Estimates from seasonal gas cycles in the upper ocean near Bermuda. *Journal of Marine Research*, **47**, p. 169–196.

STOMMEL, H. and F. SCHOTT, 1977: The Beta Spiral and the determination of the absolute velocity field from hydrographic station data. *Deep-Sea Research*, **24**, p. 325–329.

ZHANG, J., R. W. SCHMITT and R. X. HUANG, 1998: Sensitivity of the GFDL Modular Ocean Model to parameterization of double-diffusive processes. *Journal of Physical Oceanography*, **28**, p. 589–605.

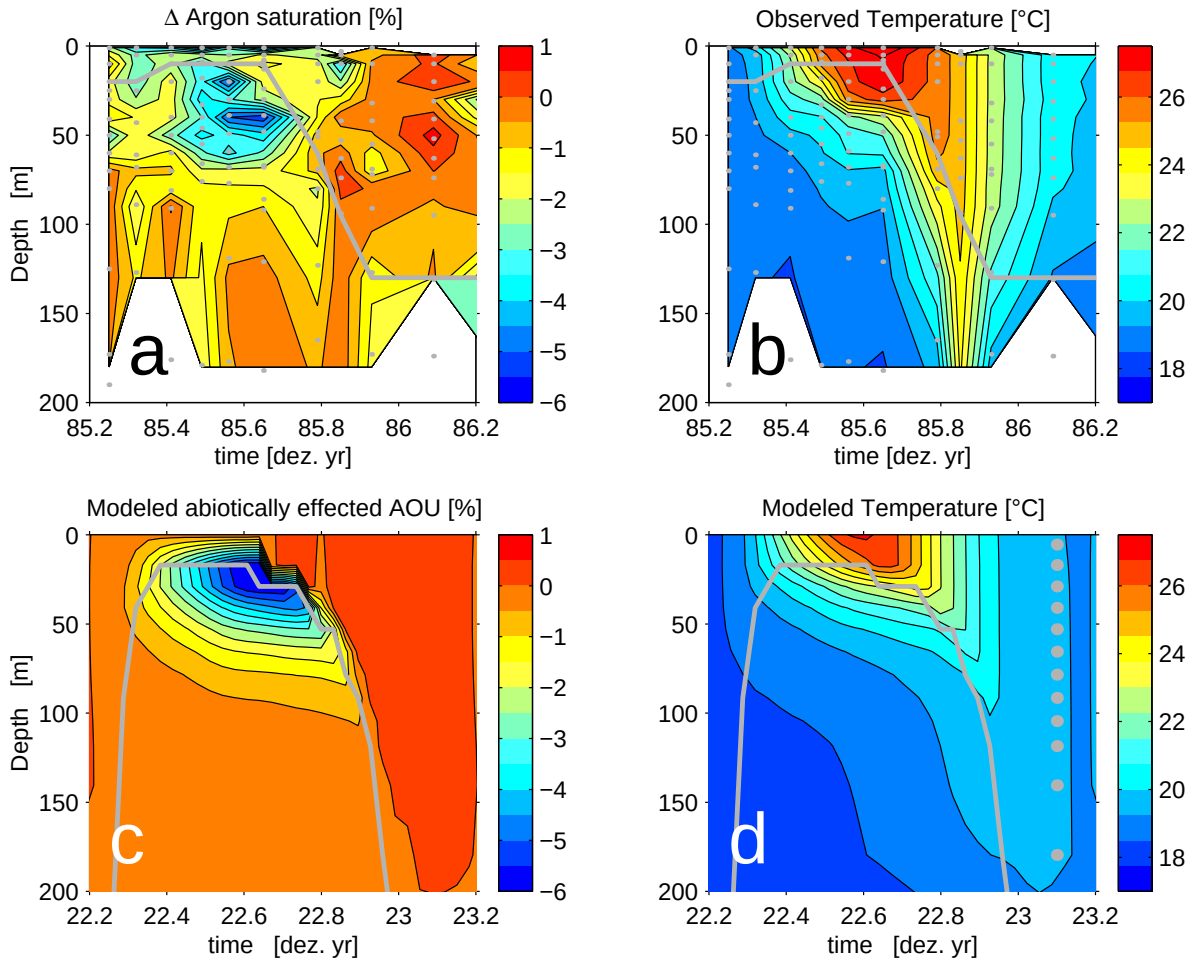

Fig. 6 (a) deviation from saturation of argon dissolved. Negative numbers denote oversaturation observed by Spitzer and Jenkins (1989) at station S. (b) temperature observed at station S. Grey dots refer to respective samples. (c) & (d) abiotically induced AOU and temperature modeled at station S. Grey dots in (d) denote vertical model grid. Grey lines indicate mixed-layer depth, here defined as the depth where density σ_0 is 0.125 higher than the density at the surface. In the model, the mixed layer reaches about 260 m.

High rates of nitrogen fixation and DOC subduction in the subtropical North Atlantic Ocean

P. Kähler, A. Oschlies, H. Dietze, B. Mourino, M. Sandow and U. Struck

To be re-submitted

High rates of nitrogen fixation and DOC subduction in the subtropical North Atlantic Ocean

Paul Kähler[1], Andreas Oschlies[1], Heiner Dietze[1], Beatriz Mourino[2], Marcel Sandow[1], and Ulrich Struck[3]

[1]*Institut für Meereskunde, Düsternbrooker Weg 20, D-24105 Kiel, Germany*
[2] *Universidade de Vigo, Departimento de Ecologia y Biologia Animal, 36200 Vigo, Spain*
[3] *GeoBio-Center^{LMU}, Richard-Wagner-Straße 10, D-80333, München, Germany*

Exceptionally high rates of nitrogen fixation reaching 4.5 mmol N per square metre and day were determined by $^{15}N_2$ uptake experiments in the oligotrophic subtropical North Atlantic Ocean. In samples of highest nitrogen fixation, this was equivalent of a daily renewal of a quarter of the particulate organic nitrogen stock. Concomittant primary-production measurements by $^{14}CO_2$ uptake yielded low rates. C:N incorporation ratios down to 3 at these stations do not fit into the orthodox concept of production and nutrient utilization in the sea. Dissolved organic matter involvement is implied with a large share of fixed carbon and nitrogen exudated and re-incorporated into biomass from DOC and DON.

Long-term nitrogen fixation rates calculated from subsurface excess nitrate combined with published water residence times are considerably smaller, but still substantial (0.5 mmol N per square metre and day). Fixation provides approximately half of the nitrogen supplied to the euphotic zone in the study area. This, and shallow DOC export by subduction, responsible for more than half of the area's oxygen utilization, close the bulk of its hitherto enigmatic carbon-nitrogen balance.

The oligotrophic subtropical gyres of the oceans have been the focus of controversy regarding the magnitude and even the direction of their biotic contribution to the air-sea flux of carbon dioxide[1-3]. Measurements of primary production and respiration, local in space and on timescales of hours, have yielded much lower biological carbon dioxide uptake (and even implied net CO_2 release) in the upper ocean, than estimates of export production from large-scale and long-term integrals of respiration in subsurface water[4,5].

In oceanic organic-matter budgeting, net production is commonly calculated from nitrate consumption, or nitrate supply to surface water – a simplified adaption of the new production concept[6]. To transform nitrogen units into carbon units, the Redfield ratio (moles C:N=106:16)[7] is widely used. Budgets of both elements composed in this way are not always consistent, especially in the oligotrophic ocean. The term carbon overconsumption has been coined for carbon uptake higher than the Redfield-ratio equivalent of consumed nitrate[8,9]. Excess carbon fixation and export, e.g. as carbon-rich dissolved organic matter[10,11], can cause carbon overconsumption, so can the utilization of unaccounted-for nitrogen. Taking nitrate for total new nitrogen excludes nitrogen sources such as dissolved organic nitrogen (DON), or N_2 via nitrogen fixation.

The mismatch between organic-matter production and nitrate supply is a general, and as yet

unexplained, problem in the subtropical North Atlantic Ocean[12,13]. It is epitomized in an area known as the "beta triangle" (Fig 1) where it was first described. There, oxygen utilization rates in subsurface water ascribed to the remineralization of organic matter exported from surface water, imply that "surface fixation of carbon … is many times greater than deduced from ^{14}C assimilation techniques"[4]. Also nitrate supply into the surface falls short of the needs of a corresponding production in this region. Oxygen utilization rates (OUR) imply a production equivalent of 0.63 mol $m^{-2}a^{-1}$ nitrogen utilization[4,5], but diffusive nitrate supply was estimated at 0.05 mol $m^{-2}a^{-1}$ only[14,15]. This leaves an unexplained gap of almost 0.6 mol N $m^{-2}a^{-1}$. We set out to investigate possible solutions to this enigma. On two cruises (Fig. 1), organic matter, nutrient, and oxygen analyses as well as incubation experiments were performed to study additional nitrogen sources for, or excess carbon from, production.

Apparent oxygen utilization (AOU) along the 2002 Section is given in Fig 2a. Combining its isopycnal gradients with gradients of water-mass age in the same area[5] yields an OUR of 5.9±0.9 mol $O_2 m^{-2}a^{-1}$ (Tab. 1). This is under the assumption that the respective data sets reflect similar physical states of the ocean, which appears reasonable in view of the similar outcome (OUR was 5.7 in [5]). Several modes of nitrogen input were considered to explain the estimated OUR. First, diffusive nitrate supply to the surface may be underestimated by state-of-the-art methods. Eddies thought to effectively inject nitrate into the surface[16] contribute but 0.05 mol $m^{-2}a^{-1}$[17]. Accounting for double diffusion, vertical diffusive nitrate input was adjusted upward by a factor of two to 0.1 mol $m^{-2}a^{-1}$[18] compared to previous estimates[14]. Vertical and horizontal advection and horizontal diffusive fluxes result in a maximal additional net nitrate input of 0.07 mol $m^{-2}a^{-1}$[18]. Adding up all physical nitrate transports to the surface leaves a nitrogen gap of >0.4±0.15 mol $m^{-2}a^{-1}$.

N_2 uptake experiments using the tracer $^{15}N_2$ yield ongoing rates of nitrogen fixation, which was measurable in all experiments; in some cases rates were extremely high (Fig. 3a-c). Rates as high as measured at three (of three, Fig. 3a) stations in April 2001 and at one (of four, Fig 3b and c) stations in March 2002 are unprecedented in the open ocean. Concomittant measurements of primary production by the ^{14}C technique yielded low rates in all cases (Fig. 2a-c). Where nitrogen fixation was high the ratio of C and N incorporation was therefore unusually low (Tab. 2).

The natural abundance of ^{15}N in particulate organic matter can be used to estimate the proportions of N_2 and NO_3 as nitrogen sources, since both have distinctly different ^{15}N contents. Taking the $\delta^{15}N$ as -2 for the nitrogen from nitrogen fixation and of 4.5 for that from nitrate uptake[19] an average 50% share of fixation-derived nitrogen in organic particles is obtained (Fig. 3d), it diminishes with depth where nitrate utilization gains importance. The small-sized fraction isolated using a 5µm pre-filter contained systematically higher shares of fixation-derived N than the bulk (Fig 3e). While until recently nitrogen fixation in the open ocean has been ascribed exclusively to large species of the genus *Trichodesmium*[20], there is nitrogen-fixing potential also in oceanic pico-cyanobacteria[21]. The pronounced ^{15}N depletion of small particles suggests them to be important in the study area. Visible *Trichodesmium* colonies were only occasionally encountered during our cruises and were absent at the stations of high nitrogen fixation.

Particulate organic matter in surface water had a N:P ratio far greater than the Redfield N:P ratio of 16 (Fig. 3f), indicative of the presence of N_2 fixing organisms, which have been

reported to be high in N:P[22]. Also this proxy of nitrogen fixation decreases with depth. Excess subsurface nitrate from the export and breakdown of organic matter high in N:P can be used to quantify the effect of nitrogen fixation[23]. We define excess nitrate as

$$NO_{3(excess)} = NO_3+NO_2-16*PO_4 \qquad (1)$$

(i.e. include NO_2, but neglect ammonium which was unimportant). It is implicitly assumed that interannual variation in preformed inorganic N:P ratios is negligible and, in the well-oxygenated water in question there is no denitrification which would decrement (1). A plot of fixation-derived nitrogen calculated in this way is given in Fig 2b. A region of $NO_{3(excess)}$ is observed in the oligotrophic centre of the studied transect between 150 and 400m. The rate of excess-nitrate buildup (analogous to the OUR estimate) representing the long-term rate of nitrogen fixation, is 0.19±0.06 mol N m^{-2} a^{-1}, or 0.52 mmol $m^{-2}d^{-1}$ (Tab. 1). In a similar approach using basin-wide excess nitrate combined with CFC water age the eastern part of the subtropical gyre (i.e. our study area) turned out a prominent source of fixed nitrogen for the North Atlantic[24].

Total organic nitrogen (TON) contributed to excess nitrate. Surface TON concentration dropped from 7.7 to 6.4 $mmolm^{-3}$ between 31.5° and 22.9°N. With a mean surface current of 4.8 cms^{-1} heading south, this would correspond to a TON consumption along the transect of 0.08 $molm^{-2}a^{-1}$ in the Ekman layer (ca. 40m) if the TON gradient were permanent. This, however, is unlikely. TON during summer was as low as 6.5 $mmolm^{-3}$ at 33°;N°22W[11]. Surface TOP (total organic phosphorus) was constant over the same distance at 0.15, to rise to 0.33 $mmolm^{-3}$ only further south. Dissolved organic matter thus contributed an excess of N over P. Whether the excess TON is itself derived from nitrogen fixation, and for how long its gradient exists, is not known. Its effect is included in the excess nitrate analysis.

Apart from extra nitrogen supply, also excess carbon export by subduction of TOC (total organic carbon)[25] contributes to close the apparent C-N imbalance. Fig. 2c gives TOC concentrations. Analyzing the isopycnal loss of TOC in the same way as the OUR and $NO_{3(excess)}$ gain, yields a rate of TOC breakdown of 2.9 mol $m^{-2}a^{-1}$ (Tab. 1). It dominates in the density range of σ_θ=26.2 and 26.35, i.e. down to 200m only, and is insignificant below (Fig. 2c and Tab. 1). The TOC thus exported is associated with organic nitrogen (TON). The C:N ratio of this export is the quotient of the TOC and TON concentration differences between source and sink locations, which was 15 between 31.5 and 22.9°N. It is with this C:N ratio that total organic matter export and decomposition contributes to the buildup of remineralizatuion products, a reflection of the participitation of N-poor dissolved organic matter[10,11]. This C:N ratio corresponds to a $C:O_2$ ratio of -1.1rather than the Redfield ratio of -1.3. Total organic matter export by subduction explains slightly more than half the oxygen consumption along the 2002 (-3.2 $molm^{-2}$ O_2.)

Summarizing (all numbers in this paragraph are mol $m^{-2}a^{-1}$ of the respective element): A variety of processes contribute to the solution of the apparent C-N imbalance in the subtropical North Atlantic. Two processes dominate: The subduction and breakdown of C rich dissolved organic matter accounts for more than half the subsurface oxygen consumption (-3.2 of -5.9 O_2). Nitrogen fixation (including surface DON loss of 0.08 N), estimated from excess nitrate, supplies about half the new nitrogen (0.19 N). The other half (<0.22 N) is from nitrate inputs by eddy (0.05 N) and double-diffusion enhanced (0.1 N) nitrate supply to the

euphotic zone and net nitrate advection (<0.07 N). Nitrogen fixation determined experimentally during two springtime cruises are in the range of the long-term estimate and far above. Adding up all considered contributions, after converting total nitrogen inputs (<0.41N) and oxygen consumption not attributible to TOC breakdown (-2.7 O_2) into carbon using the Redfield ratio, the balance is <0.6 C. The gap which we set out to explain is "overexplained" by ca. 15%. Given the errors associated with each estimate this is tolerable. The surplus is likely to be due to export to depths greater than 405m.

The high proportion of nitrogen fixation vs. primary production at the 2001 Stations can be explained by characteristics of the methods employed, which measure incorporation into the particulate phase. If, however, the bulk of fixed C and N were exudated, a large DOC pool would dilute ^{14}C more than a small DON pool would dilute ^{15}N. Uptake from the dissolved organic pool would consequently shift the ^{14}C:^{15}N ratio to low values. With bacteria as DOM utilizers, this would affect especially the small size fractions, in agreement with observations. High DON exudation rates of N_2 fixing cyanobacteria[26], and DON consumption, but high DOC surface accumulation in the study area (Fig. 2c) support this explanation. The magnitude of nitrogen fixation in the oligotrophic ocean thus appears to be intimately linked with the dynamics of dissolved organic matter. Both dominate C and N cycling at our study site. What controls either remains among the major open questions of contemporary ocean biogeochemistry. Any attempt to understand or even predict the biota's contribution to the air sea exchange of CO_2 in the subtropical ocean will be futile without this knowledge.

Methods: Nutrients were measured by standard protocols[27] using an autoanalyzer, particulate C and N by C/N analyser (Heraeus), particulate P and total dissolved P photometrically after persulfate digestion[27], TOC and TON by high-temperature oxidation[28], oxygen by Winkler titration[27] with optical endpoint determination (WOCE standard; SIS instruments). $^{15}N_2$ incubations and calculations related to ^{15}N natural abundance were according to [29]. The suspicion that the Nitrogen fixation rates are artifacts due to $^{15}NH_4^+$ uptake from ammonia-contaminated $^{15}N_2$ gas used in the experiments (Abell pers.comm.) could be dismissed (but gross NH_3 contamination was found in a $^{15}N_2$-bottle not used). $\delta^{15}N$ measurements were performed using an automated continuous-flow analyzer system (Thermo Finnigan Delta *plus* connected to a Thermo CN 2500 CHN-Analyzer). Primary production was determined by the ^{14}C method[2].

FIGURE CAPTIONS

Fig. 1: Cruise tracks and station map. The triangle is the ß-triangle of[4,5].

Fig 2: Latitudinal sections of properties along 30°W. a: Apparent oxygen utilization (AOU, mmol O_2 m^{-3}), b: Excess nitrate ($NO_{3(excess)}$, mmol N m^{-3}), c: total organic carbon (TOC, mmol C m^{-3}).

Fig 3: a -c: measured rates of N_2 and CO_2 incorporation into particles (nitrogen fixation and primary production) in April 2001 (a) and March 2002 (b,c; note different scales for nitrogen fixation!), d,e: estimated shares of fixation-derived particulate organic nitrogen (PON) for (d) all samples of 2001 Transect, and (e) all samples from incubation stations in 2002, PON (.) and in size fraction <5µm (large symbols); f: N:P ratios in particulate organic matter, includes all samples of 2002 Transect.

REFERENCES

1 Williams, P.J.LeB.. The balance of plankton respiration and photosynthesis in the open oceans. *Nature* **394**, 55-57 (1998)

2 Serret, P., C. Robinson, E. Fernandez, E. Teira, and G. Tilstone, 2001: Latitudinal variation of the balance between plankton photosynthesis and respiration in the eastern North Atlantic. *Limnol. Oceanogr.* **46**, 1642-1652.

3 del Giorgio P. A., Duarte C. M. Respiration in the open ocean. *Nature* **420**, 379-384 (2002)

4 Jenkins W.J. Oxygen utilization rates in North Atlantic subtropical gyre and primary production in oligotrophic systems. *Nature* **300**, 246-248 (1982)

5 Jenkins W.J. ^{3}H and ^{3}He in the Beta Triangle: Observations of gyre ventilation and oxygen utilization rates. *J. Phys. Oceanogr.* **27**, 763-783 (1987)

6 Dugdale R.C., Goering J.J. Uptake of new and regenerated forms of nitrogen in primary productivity. *Limnol.Oceanogr.* **12**: 196-206 (1967)

7 Redfield A.C, Ketchum B. H., Richards F.A. The influence of organisms on the composition of seawater. in: M.N. Hill (ed.), *The Sea* 2, 26-77 (1963)

8 Toggweiler, J. R., 1993. Carbon overconsumption. *Nature* **363**, 210-211.

9 Sambrotto, R. N., Savidge, G., Robinson, C., Boyd, P., Takahashi, T., Karl, D. M., Langdon, C., Chipman, D., Marra, J., Codispoti, L., 1993. Elevated consumption of carbon relative to nitrogen in the surface ocean. *Nature* **363**, 248-250.

10 Emerson S. and T.L. Hayward (1995): Chemical tracers of biological processes in shallow waters of the North Pacific: Preformed nitrate distributions. *Journal of Marine Research* **53**, 499-513

11 Kähler, P. and W. Koeve (2001): Dissolved organic matter in the ocean: Can its C:N ratio explain carbon overconsumption? *Deep-Sea Research I* **48**, 49-62

12 Michaels, A.F., N.R. Bates, K.O. Buesseler, C.A. Carlson, K.A. Knap (1994): Carbon system imbalances in the Sargasso Sea. *Nature* **372**, 537-540

13 Lipschultz, F., N.R. Bates, C.A. Carlson, D.A. Hansell, 2002, New production in the Sargasso Sea: History and current status. *Global Biogeochemical Cycles* **16**, 1-17

14 Lewis, M. R., W. G. Harrison, N. S. Oakey, D. Herbert, and T. Platt (1986): Vertical nitrate fluxes in the oligotrophic ocean. *Science* **234**, 870-873

15 Oschlies, A., 2002a: Nutrient supply to the surface waters of the North Atlantic – a model study. *J. Geophys. Res.* **107**, 10.1029/2000JC000275

16 McGillicuddy, D. J. Jr., A. R. Robinson, D. A. Siegel, H. W. Jannasch, R. Johnson, T. D. Dickey, J. McNeil, A. F. Michaels, and A. H. Knap, 1998: Influence of mesoscale eddies on new production in the Sargasso Sea. *Nature* **394**, 263-266

17 Oschlies, A., 2002b: Can eddies make ocean deserts bloom? *Global Biogeochem. Cycles*, in press

18 Dietze, H., A. Oschlies, and P. Kähler, 2003, Internal-wave induced and double-diffusive nutrient fluxes to the nutrient-consuming surfce layer in the oligotrophic subtropical North Atlantic. *Ocean Dynamics*, submitted

19 Montoya J.P., E.J. Carpenter, D.G. Capone, 2002. Nitrogen fixation and nitrogen isotope abundances in zooplankton of the oligotrophic North Atlantic. *Limnology and Oceanography* **47**, 1617-1628

20 Capone, D. G., J. P. Zehr, H. W. Paerl, B. Bergman, and E. J. Carpenter, 1997: *Trichodesmium*, a globally significant marine cyanobacterium. *Science* **276**: 1221-1229.

21 Zehr, J. P., J. B. Waterbury, P. J. Turner, J. P. Montoya, E. Omoregie, G. F. Steward, A. Hansen, and D. M. Karl, 2001: Unicellular cyanobacteria fix N_2 in the subtropical North Pacific Ocean. *Nature* **412**, 635-638.

22 Karl, D.M., R. Letelier, V. Hebel, D.F. Bird, C.D. Winn (1992): Trichodesmium blooms and new nitrogen in the North Pacific Gyre, p 219-237. In E.J Carpenter, D.G. Capone, and J. G. Rueter (eds.) *Marine pelagic cyanobacteria: Trichodesmium and other diazotrophs.* Kluwer Academic

23 Gruber N. and J. L. Sarmiento, 1996, Global patterns of marine nitrogen fixation and denitrification. *Global Biogeochem. Cycles* **11**, 235-266

24 Hansell D.A., Bates N.R, Olsen D.B., 2003. Excess nitrate and nitrogen fixation in the North Atlantic. *Mar.Chem.* in press

25 Doval M., Hansell D.A. Organic carbon and apparent oxygen utilizationin the western South Pacific and central Indian Oceans. *Mar.Chem.* **68**, 249-264 (2000)

26 Bronk D.A., 2002, Dynamics of DON. In: *Biogeochemistry of Dissolved Organic Matter* (D.A. Hansell and C.A. Carlson, eds.) Academic Press, Amsterdam, 153-247

27 Grasshoff K., M. Ehrhardt and K. Kremling (1983): *Methods of Seawater Analysis.* Verlag Chemie, Weinheim, 419pp.

28 Kähler, P., P. K. Bjørnsen, K. Lochte and A. Antia (1997): Dissolved organic matter and its utilization by bacteria during Spring in the Southern Ocean. *Deep-Sea Res. II* **44**, 341-353

29 Montoya J.P., M. Voss, P. Kähler, and D.G.Capone, 1996. A simple, high-precision, high-sensitivity tracer assay for Nitrogen fixation. *Applied and Environmental Microbiology* **62**, 986-993

Fig. (1)

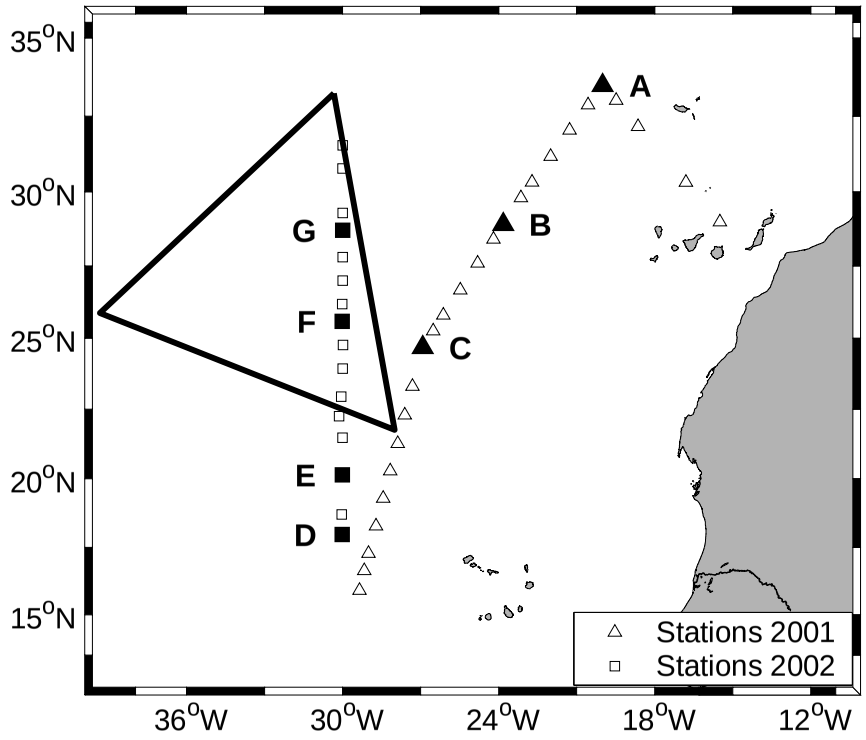
35°N
30°N
25°N
20°N
15°N
36°W
30°W
24°W
18°W
12°W
A
B
C
D
E
F
G
Stations 2001
Stations 2002

Fig. (2)

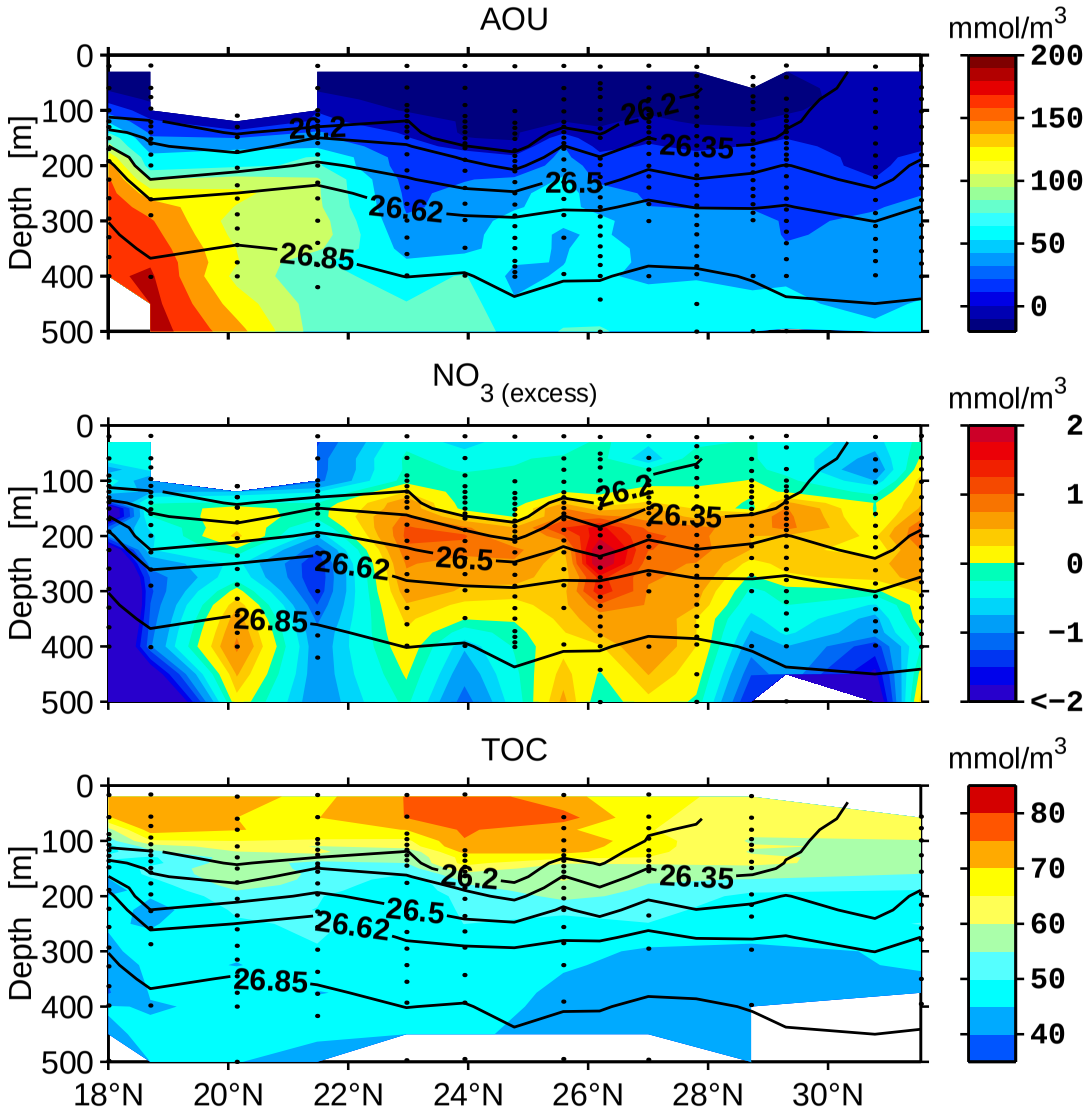
AOU
mmol/m3
200
150
100
50
0
Depth [m]
0
100
200
300
400
500
26.2
26.35
26.5
26.62
26.85
NO3 (excess)
mmol/m3
2
1
0
−1
<−2
TOC
mmol/m3
80
70
60
50
40
18°N
20°N
22°N
24°N
26°N
28°N
30°N

Fig. (3)

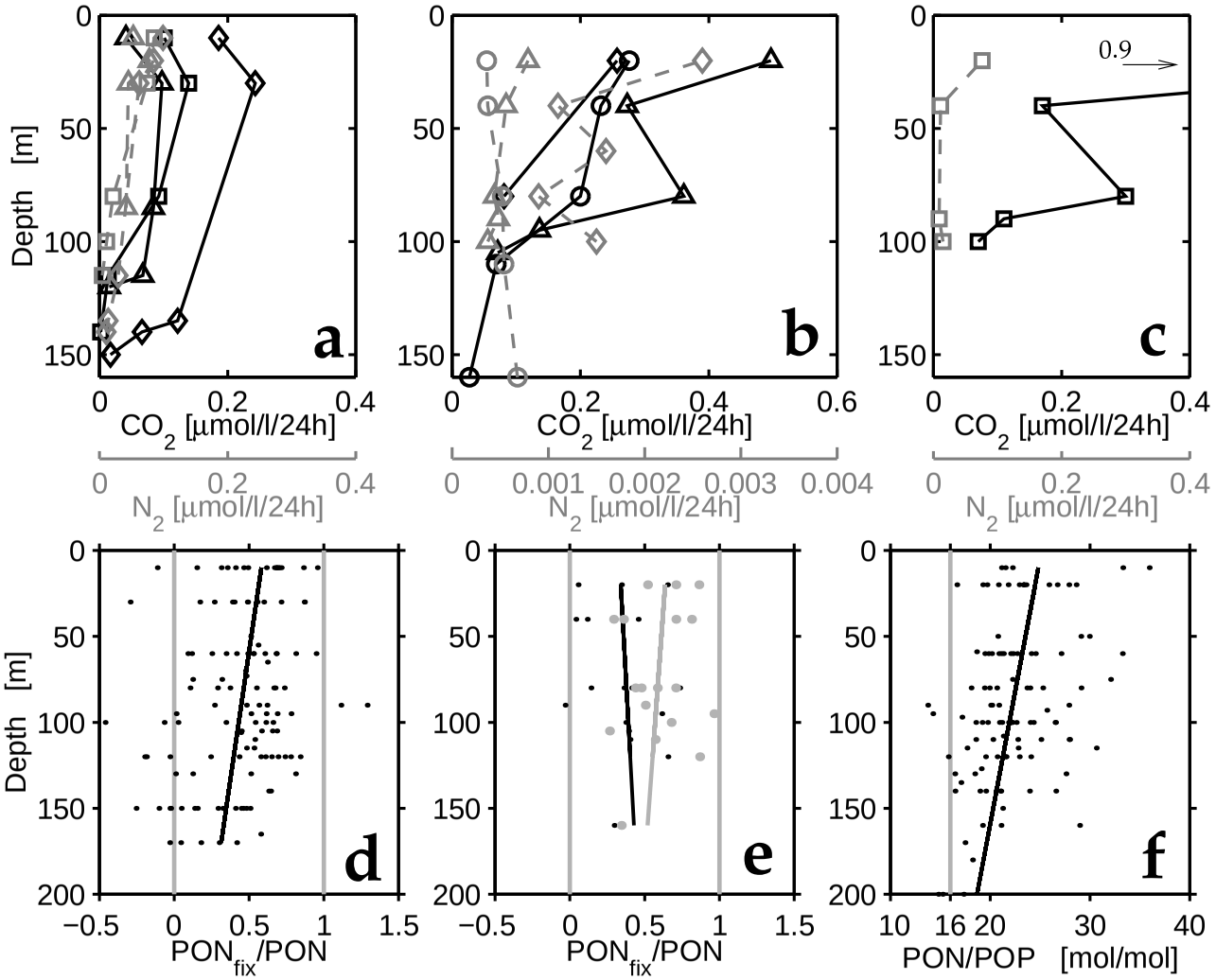
Depth [m]
0
50
100
150
200
a
b
c
d
e
f
0.9
CO2 [µmol/l/24h]
N2 [µmol/l/24h]
PONfix/PON
PON/POP [mol/mol]

Tab. 1: Long-term regional rates from isopycnal analyses

σ_0	Δlatitude	mean depth	Δτ	ΔAOU	$\Delta AOU \Delta\tau^{-1}$	ΔNO_{3xs}	$\Delta NO_{3xs} \Delta\tau^{-1}$	ΔTOC	$\Delta TOC \Delta\tau^{-1}$
kgm^{-3}	°N	m	a	$mmolm^{-3}$	$mmolm^{-3}a^{-1}$	$mmolm^{-3}$	$mmolm^{-3}a^{-1}$	$mmolm^{-3}$	$mmolm^{-3}a^{-1}$
26,20	27.0 - 22.9	120	0,15	17,2	115	0,30	2,0	-12,0	-80
26,35	29.3 - 22.9	160	0,20	10,0	50	0,40	2,0	-5,6	-28
26,50	31.5 - 22.9	210	1,40	14,8	11	0,35	0,25	-0,4	-0,3
26,62	31.5 - 22.9	270	2,00	12,5	6,3	0,49	0,25	-	-
26,85	31.5 - 22.9	405	2,75	10,1	3,7	0,91	0,33	-	-
			error	1,4		0,1		2,8	
			integral 120-405m		6,0		0,19		2,9

Along 2002 Section (Fig. 1, 2). Concentrations were interpolated to isopycnals, regressed, and differences over latitude range determined. Error from reproducability of measurements, cumulative for endpoints of regression. Age difference ($\Delta\tau$) from [5].

Tab. 2: Short-term local rates from incubations

Station	A	B	C	D	E	F	G
CO_2 uptake mmol C $m^{-2}d^{-1}$	11,3	10	27,2	44,6	35,4	15,7	23,7
N_2 uptake mmol N $m^{-2}d^{-1}$	2,8	3,3	4,5	2,7	0,27	0,71	0,26
C:N of CO_2 and N_2 uptake	4	3	6	16,5	131	22	91

Seperating physically and biotically effected air-sea fluxes of O_2 in the North Atlantic. An easy task?

H. Dietze and A. Oschlies, 2004
Submitted to Journal of Geophysical Research

Separating physically and biotically effected air-sea fluxes of O_2 in the North Atlantic. An easy task?

H. Dietze and A. Oschlies

Leibniz-Institut für Meereswissenschaften an der Universität Kiel, Kiel, Germany

Abstract. The solubility of gases in seawater is a function of temperature. Regarding an abiotic ocean (or an inert gas) it is generally assumed that, set by this relation, air-sea gas fluxes are correlated with air-sea heat fluxes as long as the gas exchange works sufficiently fast. This correlation is often used to distinguish between physically and biotically inferred oxygen fluxes, i.e. the solubility pump and the biological oceanic pump. Integrations of an eddy permitting, coupled 3-D circulation-oxygen model of the North Atlantic indicate that this method, if applied regionally, is of limited success. In addition we report significant outgassing at the equator which might well be a model artefact endemic to state-of-the-art z-level biogeochemical ocean models.

1. Introduction

Neglecting all mechanisms that can produce deviations from saturation of a gas dissolved in seawater results in a tight coupling between air-sea heat flux Q and gasflux F:

$$F = -\frac{\partial C^{sat}}{\partial T}\frac{Q}{c_p}, \quad (1)$$

where $\partial C^{sat}/\partial T$ is the temperature derivative of the solubility of the respective gas and c_p is the heat capacity of sea water.

Since the air-sea exchange of oxygen is relatively fast (typical mixed layers equilibrate within days) it has become common practice to use this relation to distinguish between thermally and biotically inferred air-sea fluxes of oxygen (e.g. Ganachaud and Wunsch [2002], Keeling et al. [1998], Keeling and Shertz [1992], Gruber et al. [2001], Bopp et al. [2002], Najjar and Keeling [2000]). On the other hand it is known that abiotic processes other than finite gas exchange are capable of producing deviations from saturation in the ocean:

1. Based on measurements of argon whose physical properties are close to those of oxygen, Spitzer and Jenkins [1989] reported an annual cycle of subsurface supersaturation in the subtropics. In spring / summer water below the mixed layer is heated by solar radiation. As it warms, solubility decreases and, as it is shielded from the atmosphere, oversaturation evolves. During autumn / winter, when the mixed layer deepens due to destabilizing surface buoyancy fluxes, the oversaturated water gets back into contact with the atmosphere.

2. Due to the nonlinear relationship between oxygen saturation (i.e. solubility) and temperature, mixing of two water parcels with different temperatures and salinities does always result in a mixed parcel being oversaturated relative to the mean saturation of the original parcels (Fig. 1). Wherever such a water parcel which was subject to intense mixing gets into contact with the atmosphere, more O_2 will outgas than predicted by the oxygen-to-heat flux relation (Eq. 1). Although the resulting oversaturation is small (0.9% in the example illustratet in Fig. 1) it might well effect air-sea oxygen fluxes of an order of magnitude comparable to typical oxygen production rates from annual net community production (e.g. 200 m deep winter mixed layer oversaturated by 0.9% regaining contact with the atmosphere potentially looses 1 mol O_2/m^2 excess while typical biotically effected O_2 fluxes correspond to 2 mol O_2/m^2/a (Oschlies and Kähler [2004])).

This model study examines the potential of solar radiation penetrating beneath the mixed layer and mixing to decouple air-sea heat and oxygen fluxes in an abiotic ocean.

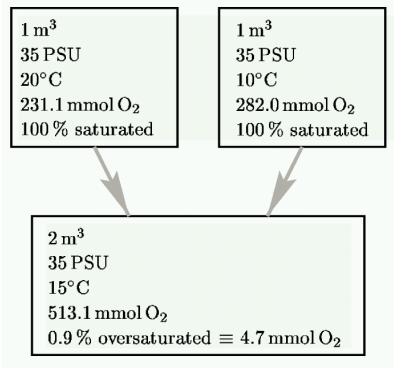

Figure 1. Mixing of two water parcels with different temperatures results in a mixed parcel oversaturated relative to the mean oxygen saturation of the original parcels.

2. Method

An oxygen compartment, treated like an inert gas (e.g. argon), is embedded (on-line) into a 2/5° × 1/3° resolution circulation model of the North Atlantic. The turbulence closure scheme used was shown to adequately simulate the seasonal mixed-layer cycle and diffusion in the main thermocline (Oschlies et al. [2000]). Numerical advection and diffusion schemes are capable of reproducing results of the Ledwell et al. [1998] tracer release experiment (Eden and Oschlies [2003 subm.]).

The atmospheric forcing consists of monthly mean windstress and heat flux fields derived from the years 1989-1993 of the reanalysis project carried out at the European Centre for Medium-Range Weather Forecasts (ECMWF) (Gibson

0148-0227/04/$9.00

ET AL. [1997]). Freshwater fluxes are parameterized by restoring surface salinity to observed monthly means taken from the LEVITUS ET AL. [1994] atlas. The formulation of the surface heat flux follows HANEY [1971]. Solar heat flux penetrates into the ocean. Absorbtion is parameterized using the water type I of JERLOV [1976].
All simulations were integrated for 20 years starting from a common spin-up state of the circulation model and oxygen concentrations corresponding to 100% saturation. Oxygen is reset to 100% saturation every timestep ($\approx$ 30 minutes) at the restoring zones of the circulation model (Fig. 6).
Air-to-sea oxygen flux FO_2 is modeled following the OCMIP-2 (R. G. Najjar and J. C. Orr, Design of OCMIP-2 simulations of chlorofluorocarbons, the solubility pump and common biogeochemistry, 1998; available from the World Wide Web at http://www.ipsl.jussieu.fr/OCMIP) guideline or stated differently:

$$FO_2 = KW \left(O_2^{sat} - O_2^{surf}\right) \quad (2)$$

where O_2^{sat} is the oxygen concentration corresponding to a 100% saturation according to GARCIA AND GORDON [1992],

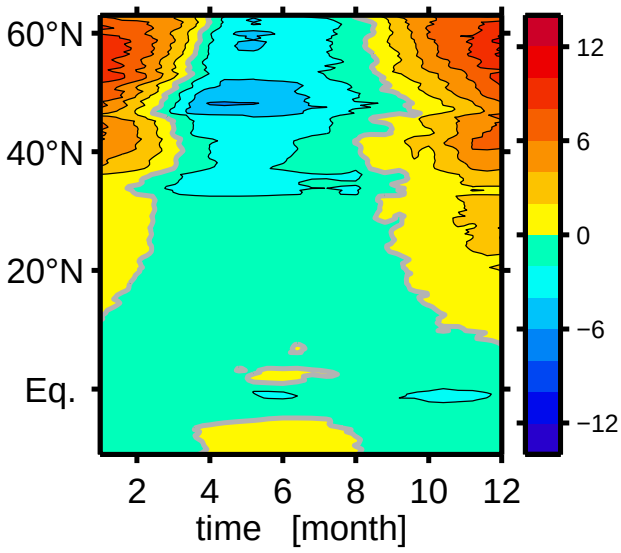

Figure 2. Zonal mean of modeled abiotically induced air-sea oxygen flux. Units are $mol\,O_2\,m^{-2}\,a^{-1}$, negative numbers denote oceanic oxygen-uptake. Subsurface heating due to solar radiation is parameterized using Jerlov's water type I.

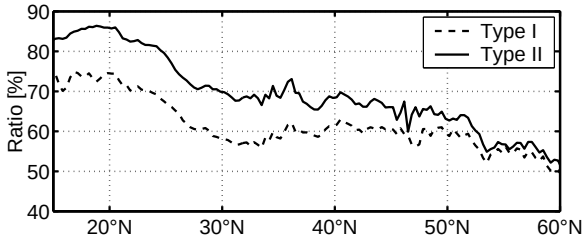

Figure 3. Zonally averaged seasonal amplitudes of modeled air-sea oxygen fluxes relative to amplitudes derived from heat fluxes following equation (1). Type I and II refer to Jerlov's optical water types used to parameterize subsurface heating due to solar radiation in the respective model integrations.

O_2^{surf} is oxygen concentration in the uppermost grid box and KW is the piston velocity, calculated according to:

$$KW = a\,(u2 + v)\,(ScO_2/660)^{-1/2} \quad (3)$$

with coefficient $a = 0.337/3.610^5$s/m and the Schmidt number of oxygen in seawater ScO_2 as a function of temperature as proposed by KEELING ET AL. [1998]. The square of monthly mean wind speed $u2$ and the variance v of wind speed computed over one month were calculated from ECMWF climatology (using the same database which drives the circulation model). A crude ice model switches off air-to-sea oxygen fluxes whenever sea-surface temperatures drop below -1.8°C.
Processes that change oxygen saturation are quantified by calculation of apparent oxygen utilisation fluxes FAOU. In this study apparent oxygen utilisation (AOU) refers to deviations from saturation due to physical processes rather than due to net biotic respiration. Apparent oxygen utilisation fluxes $FAOU_{mech}$ due to respective transport mechanisms $mech$ are calculated according to:

$$FAOU_{mech} = \frac{\partial O_2^{sat}}{\partial T}\frac{Q_{mech}}{c_p} + \frac{\partial O_2^{sat}}{\partial S} FS_{mech} - FO_{mech} \quad (4)$$

where $\partial O_2^{sat}/\partial T$ and $\partial O_2^{sat}/\partial S$ are temperature and salinity derivatives of the solubility of oxygen. c_p is the heat capacity of sea water, Q_{mech}, FS_{mech}, FO_{mech} are heat, salt and oxygen flux, respectively. This study distinguishes between AOU production due to horizontal ($FAOU_{ah}$) and vertical ($FAOU_{av}$) advection, horizontal ($FAOU_{dh}$) and vertical ($FAOU_{dv}$) diffusion and solar radiation penetrating beneath the surface ($FAOU_{sol}$). Note that the separation between advective and diffusive fluxes is to some extent arbitrary: Taking a Lagrangian point of view it is evident that advection can neither be a source nor a sink for AOU (i.e. deviations from saturation) while diffusion is capable of producing oversaturation due to the nonlinear relationship between the solubility of oxygen and temperature / salinity. In ocean models solving Reynolds-averaged finite-difference equations in an Eularian frame of reference the distinction between advection and diffusion is problematic. Numerically, both result in a partial mixing of adjacent boxes, dependent on gradients and flow rate / diffusivity, respectively. This means that advection in the model is not only redistributing oversaturated water, but might as well be a source of oversaturation.

3. Decoupled air-sea heat and oxygen fluxes on seasonal timescale

SPITZER AND JENKINS [1989] reported a seasonal cycle of argon supersaturation in the upper watercolumn at station BATS (32°N 64°W, Fig. 6). As argon is an inert gas, this cycle is driven solely by physical processes. A companion study (DIETZE AND OSCHLIES [2004 subm.]) showed that the seasonal cycle in supersaturation can be explained by radiative heating of subsurface water capped off the atmosphere during spring / summer and subsequent mixed layer deepening during fall / winter. It is evident that such a process decouples the relation between air-sea heat and oxygen fluxes described by equation (1). A rough calculation gives a quantitative estimate of this process:
Solubility and diffusivity of argon in seawater, as well as their dependance on temperature are close to those of oxygen. Hence argon is a good proxy for the abiotic fraction of oxygen dissolved in seawater and oxygen supersaturation caused by abiotic processes can be calculated using argon data. Using data published by SPITZER AND JENKINS [1989]

this yields a seasonal cycle in oxygen supersaturation ranging from zero in winter to $1\,mol\,O_2/m^2$ in summer (vertical integral over upper $180\,m$).
Roughly speaking the outgassing to be expected (according to equation (1)) due to warming in spring / summer is subdued by $2\,mol\,O_2/m^2/a$ as we find a supersaturation of $1\,mol\,O_2/m^2$ build up in the cause of half a year. In fall / winter the ocean is cooled but the oceanic oxygen uptake proposed by equation (1) is opposed by oversaturated water regaining contact with the atmosphere as the mixed layer deepens. Using the same argument as above yields an oceanic oxygen gain due to cooling subdued by $2\,mol\,O_2/m^2/a$.
According to DONEY [1996] net air-sea heat fluxes at the BATS site range from $-250\,W/m^2$ in winter to $150\,W/m^2$ oceanic heating in summer. Based on these numbers equation (1) proposes oxygen fluxes into the ocean of 7 and $-4\,mol\,O_2/m^2/a$ respectively. This corresponds to a seasonal amplitude of $5.5\,mol\,O_2/m^2/a$ which is, as we calculated above, subdued by $2\,mol\,O_2/m^2/a$ which are almost 40%.
In order to assess the effect of subsurface radiative heating on basin scale we use the model described in the previous section. The focus is on the subtropical gyre of the North Atlantic. There, the zonal mean of Jerlov's optical water types (JERLOV [1976]) describing downward irradiance versus depth is somewhere in between type I and type II (SIMONOT AND TREUT [1986]). Two model runs are performed. One using Jerlov's water type I, the other one with reduced penetration uses type II.
Fig. 2 shows the annual cycle of air-sea oxygen flux modeled with type I. Qualitatively the seasonal cycle of net air-sea heat flux is well reproduced: Apart from the equatorial region the ocean takes up oxygen in winter and gasses out in summer. In the vicinity of the equator the latitudional meandering of the intertropical convergence zone accounts for a weak annual cycle.
Fig. 3 shows zonally averaged seasonal amplitudes , obtained by harmonic analysis, of air-sea oxygen fluxes modeled with respective Jerlov's water types relative to oxygen fluxes derived from heat flux according to equation (1): Using Jerlov's water type I results in an air-sea oxygen flux attenuated by 43% relative to the prediction based on heat flux (equation (1)). This is consistent with the rough calculation based on argon data at the beginning of this section. Even reduced penetration of solar radiation, parameterized by Jerlov's water type II, proposes a considerable error (32%) in the subtropical North Atlantic if the seasonal cycle of abiotically induced air-sea oxygen flux is derived from heat flux alone.

4. Regionally decoupled air-sea heat and oxygen fluxes

The solubility of oxygen in seawater is a nonlinear function of temperature and salinity. The effect of temperature on solubility is an order of magnitude larger than that of salinity for the range under consideration (Fig. 4). Imagine two water parcels with a salinity of 35 PSU, a volume of $1\,m^3$ each and temperatures of $20°C$ and $10°C$ respectively. Assuming the parcels are saturated with oxygen yields a total of $513.1\,mmol\,O_2$ dissolved. Mixing the two water parcels results in a parcel of temperature $15°C$, salinity 35 PSU and a saturation concentration of $508.4\,mmol\,O_2$, so that the mixed parcel ends up with a supersaturation of $4.7\,mmol\,O_2$ (Fig. 1). Although this is a small number it may have significant impact on the interpretation of estimated air-sea oxygen fluxes:
Inversion of WOCE data yields an oceanic oxygen gain due to the combined effect of biological and solubility pump of $600 \pm 200\,kmol\,O_2/s$ between 24°N and 48°N in the North Atlantic while an estimate based on heat-flux alone (equation (1)) proposes $750 \pm 150\,kmol\,O_2/s$ (GANACHAUD AND WUNSCH [2002]). Ignoring errors and assuming that the heat flux estimate accounts for all physical processes suggests a net biotic oxygen production of $150\ kmol\,O_2/s$. Following the calculation above and assuming that the Gulf Stream, which increases from 30 Sv in the Florida Straight to 70-100 Sv at Cape Hatteras, effectively mixes 32 Sv of temperature $10°C$ with 32 Sv of temperature $20°C$ would reverse the sign of the biotic oxygen production estimate in the region.
In the following, the impact of mixing on air-sea oxygen flux is investigated in more detail in the coupled oxygen-circulation model described in section (2). In order to cancel out potential effects of radiative heating and finite gas exchange, air-sea oxygen flux is treated differently: Surface oxygen concentrations are reset to saturation every timestep. In addition an artificial subsurface oxygen flux is constructed such as it exactly compensates for supersaturation due to radiative heating. Its magnitude is calculated according to equation (1).
The modeled net oxygen uptake of the ocean is, as expected, regionally biased towards increased oceanic outgassing (Fig. 5). In the equatorial region the effect of mixing enhances oceanic outgassing by up to $0.25\,mol\,O_2/m^2/a$. At 48°N the effect is strongest, subdueing the oceanic oxygen uptake due to net oceanic heat loss by up to $0.8\,mol\,O_2/m^2/a$, so that the sign of air-sea gas exchange is reversed relative to the proposition based on heat flux. Integration between 24°N and 48°N yields a correction of $162\,kmolO_2/s$ which is more than the difference between heat-flux derived and transport-derived O_2 fluxes attributed by GANACHAUD AND WUNSCH [2002] to the biological pump. It is noteworthy that the effect of air-sea salinity flux is negligible. Its effect can be derived from (Fig. 5): Wherever evaporation exceeds precipation even the heat flux estimate corrected by the mixing term exceeds the modeled air-sea oxygen flux.
The fraction of modeled air-sea oxygen flux which is induced by mixing shows a distinct horizontal distribution (Fig. 6). Most of it is produced in the Gulf Stream, the Gulf Stream extension where the Gulf Stream mixes with the Labrador Current, and in the equatorial region.
The partition of the production of oversaturation into respective mechanisms reveals some insight into mixing processes at work (Fig. 7). Note that it is impossible to produce undersaturation by mixing. A mixed water parcel always ends up being oversaturated relative to the original parcels. Hence the only process capable of producing undersaturation is demixing, the reversed process. Fig 7 (b) shows the vertical integral of the divergence of apparent oxygen utilisation fluxes due to vertical advection. Negative values denote production of oversaturation, mirroring the mixing effect of advection explained in section (2). Positive values, i.e. production of undersaturation e.g. within the equatorial region must be inferred by demixing. This demixing is a spurious effect of the advection scheme used (central differences both in space and in time, widely-used because of conceptual simplicity, little implicit diffusion, and $O(\Delta x^2)$ accuracy). Whenever the grid Péclet number $Pe = u\,\Delta x/K$ with velocity u, grid spacing Δx and diffusivity K exceeds 2 over- and undershoots produced by numerics may often occur. The sufficient condition for the absence of spurious over- and undershoots is not satisfied in ocean general circulation models (OGCM) (e.g. OSCHLIES [1999]). Even the high resolution (1/10°) OCGM of SMITH ET AL. [2000] which is, up to date, the only z-level model of the North Atlantic that models a realistic separation of the Golf Stream at Cape Hatteras, massively violates this criterium. In their model horizontal velocities must be less than $1.3\,cm\,s^{-1}$ at

the equator and less than $0.03\,cm\,s^{-1}$ at 73° N in order to ensure grid Péclet numbers less than two.

Fig. 7 summarizes that mixing, as it occurs in a OGCM based on central differences, is a complex process involving massive numerical artefacts. Besides advection schemes, horizontal biharmonic diffusion (as employed in this model) may as well be another source of numerical dispersion (demixing) as this scheme is not positive definite. Moreover the latter effects may produce static instabilities, which in turn affect vertical diffusion schemes.

What remains is to show that the combined effect of advection and diffusion in OGCMs is realistic (which is beyond the scope of this work, but see EDEN AND OSCHLIES [2003 subm.]). While measurements of trancient tracers such as helium, tritium, CFCs and purposefully deployed SF6 have already proved to be a valuable base for model evaluation we propose that an argon climatology would be of additional benefit for the OGCM community: Wherever argon supersaturation shows up in the deep ocean, mixing must have occured if other nonadiabatic processes or bubble entrainment at the surface can be ruled out.

Fig. 8 shows a vertical section of modeled (annual mean) oxygen saturation through the North Atlantic (along the transect marked in Fig. 6). If modeled mixing rates are realistic, the effect of mixing on argon supersaturation is above measurement accuracy (at least 0.6% deviation from saturation can be resolved according to SPITZER AND JENKINS [1989]) of argon supersaturation. Fig. 8 also shows that the dispersive effects are not always canceling out, as we observe undersaturation in the Gulf Stream extension.

Quantifying the net contribution from dispersion is not straightforward, and we are not aware of a method to isolate the numerical artefacts. Nevertheless the budget calculations in Tab. 1 gives an idea concerning their magnitudes: In the "equatorial box" (Fig. 6) the effect of horizontal and vertical advection on oxygen saturation is two orders of magnitude higher than the combined effect of horizontal

Table 1. Budget of annual mean divergence of apparent oxygen utilisation fluxes within "northern" and "equatorial" box (Fig. 5). Run i refers to the standard integration of this section. In run ii saturation is reset every timestep, so that these figures explicitly represent sources and sinks of oversaturation. Units are $kmol\,O_2/s$. Negative numbers denote supersaturating effects of horizontal / vertical advection (ah, av) and horizontal / vertical diffusion (dh, dv), decreasing stock of supersaturation ($Storage$) and oceanic outgassing due to the combined effect ($\sum$).

Box	Run	ah	av	dh	dv	$Storage$	$\sum$
equat.	i	-490	475	-2	-7	< 1	-23
equat.	ii	-480	475	-1	-7	-	-
northern	i	20	-33	-45	-6	2	-62
northern	ii	27	-33	-45	-6	-	-

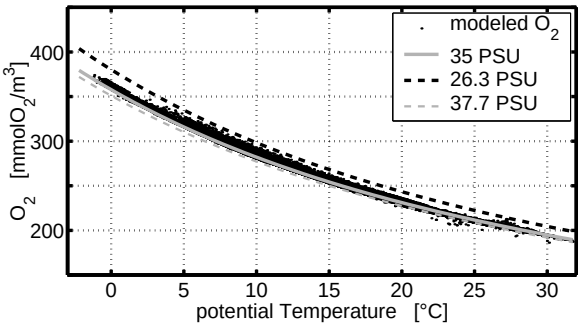

Figure 4. Solubility of oxygen as a function of temperature according to GARCIA AND GORDON [1992]. Black dashed line refers to minimum salinity found in the model domain (Amazonas inflow, where surface salinity restoring ensures low salinities). The grey line refers to salinity equal to 35 PSU and the grey dashed line to maximum salinity found in the model domain. Black dots are all oxygen concentrations found in the model, plotted versus their respective potential temperature.

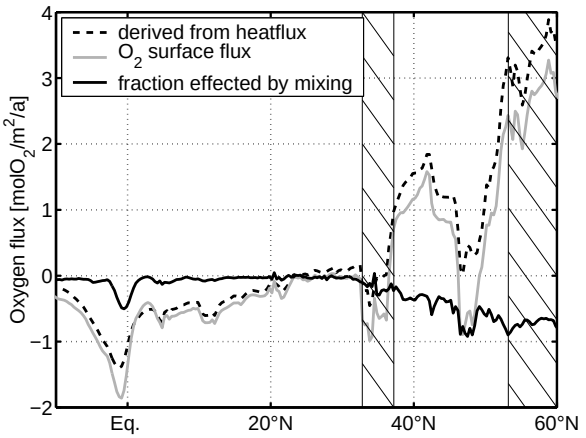

Figure 5. Zonal average of annual mean abiotically induced oxygen fluxes (positive is into the ocean): Grey line denotes the modeled air-sea flux. Dashed line is air-sea oxygen flux derived from heat flux according to equation (1). Positive values indicate oceanic oxygen uptake. Solid, black line is the fraction of modeled air-sea flux attributed to mixing. Shaded regions correspond to the latitudes of restoring zones.

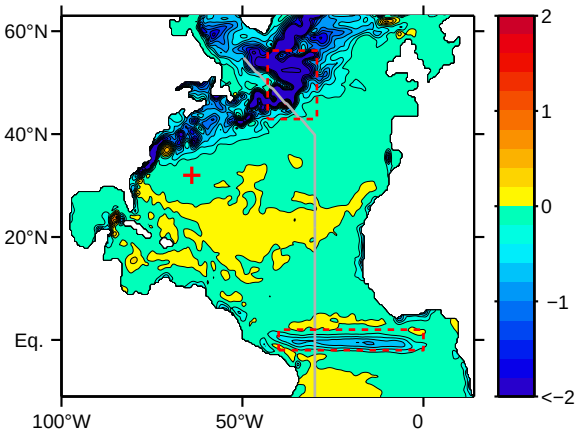

Figure 6. Fraction of modeled air-sea oxygen flux induced by mixing (annual mean). Units are $mol\,O_2/m^2/a$, negative values denote regions where oceanic outgassing is increased or oceanic oxygen-uptake is subdued by mixing. Horizontal smoothing was applied (boxcar type with a filterwidth of $\approx 1.5°$). Red cross indicates the position of station BATS. Dashed boxes bound the regions termed "equatorial" and "northern" box respectively. Grey line indicates the course of the vertical section contoured in Fig. 8. Grey patches are restoring zones near the Strait of Gibraltar and in the Labrador Sea where temperature and salinity are restored to climatological values, while oxygen is reset to saturation every timestep. Northern and southern restoring zones bounding the model domain are not shown.

and vertical mixing. The net effect on abiotic air-sea oxygen flux is basically the difference of two huge numbers of which one describes the demixing effect of vertical advection which is definitely a numerical artefact. We conclude that the enhanced equatorial outgassing due to mixing is uncertain, as it might well be the case, that spurious mixing inferred by horizontal advection overcompensates the massive demixing effect of vertical advection.
In the "northern box", where the Golf Stream mixes with Labrador Current, the spurious demixing effect of horizontal advection is an order of magnitude smaller than the demixing effect of vertical advection in the "equatorial box". So mixing processes modeled there are determined to a lesser extent by numerical dispersion.

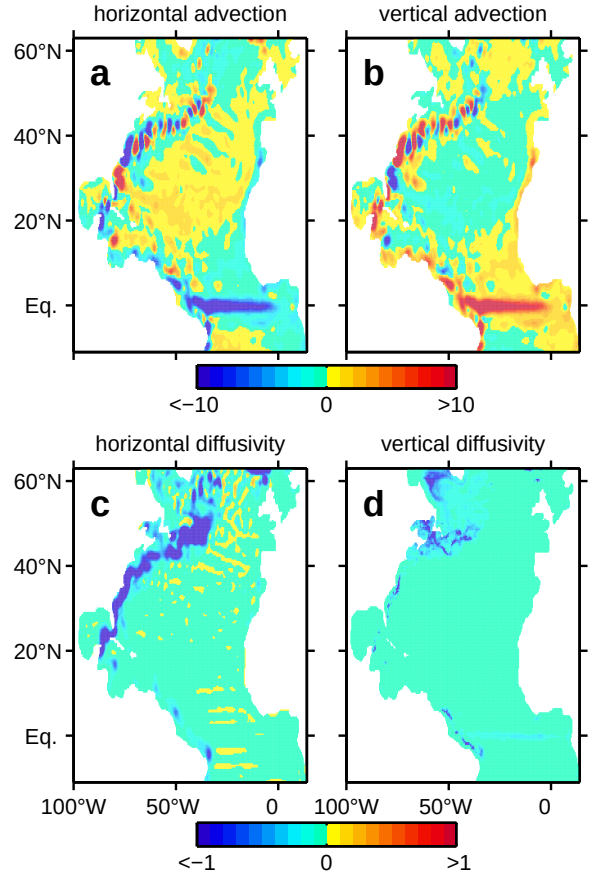

Figure 7. Vertical integrals of annual mean-divergences of apparent oxygen utilisation fluxes inferred by respective mechanisms. Units are $mol\,O_2/m^2/a$, positive values denote processes decreasing oxygen saturation. Horizontal smoothing was applied (boxcar type with a filterwidth of $\approx 1.5°$).

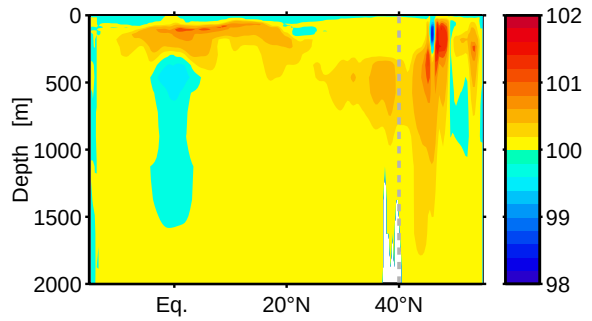

Figure 8. Section of abiotically induced annual mean apparent oxygen utilisation along the course indicated in Fig. 6. Vertical dashed line indicates change of course. Units are percent saturation.

5. Discussion

In order to draw conclusions from the model results presented here, it is crucial to assess the quality of the model. Concerning the modeled seasonal cycle of abiotically inferred air-sea oxygen flux, model evaluation is possible at a site in the subtropics (station BATS, marked in Fig. 6). For this site a companion study (Dietze and Oschlies [2004 subm.]) proved consistency between measurements of argon and modeled abiotically induced oxygen oversaturation. In addition, the amplitude of the seasonal cycle of the heat flux matches within 5% the observational estimate of Doney [1996] at station BATS.
Encouraged by these agreements we propose that estimates of the seasonal cycle in air-sea oxygen flux derived from heat flux are biased high by 20% to 40% in the subtropical North Atlantic. This applies also for all inert gases with comparable air-sea gas exchange velocities.
Validating the modeled effect of mixing on air-sea oxygen flux is a very complex task, as even the global mean of water mass transformation (which produces oversaturation) is still unknown. What we report here is that a state-of-the-art eddy-permitting model predicts significant production rates of oversaturation due to nonadiabatic mixing in various regions. Two of them, the Gulf Stream as well as its extension, are most probably sites of enhanced diapycnal mixing:
(1.) It is sensible to assume that the warm return flow of the thermohaline circulation entering the subpolar gyre mixes with cold surrounding water before or while air-sea heat fluxes increase its density so it becomes part of the deep water masses again.
(2.) Evidence of relatively high rates of diapycnal mixing in the Gulf Stream has increased up to an extent where it seems plausible that the therewith connected uplift of nutrients into the euphotic zone may be a major contribution fueling new production in the subtropical gyre of the North Atlantic (Jenkins and Doney [2003]).
The situation is somewhat different for mixing rates modeled in the equatorial region, where numerical artefacts in biogeochemical ocean models can lead to numerically generated unrealistic nitrate maxima in the eastern equatorial Atlantic (Oschlies et al. [2000]).
Correspondingly numerical effects may have an influence on simulated air-sea gas exchange of oxygen. It is noteworthy that biogeochemical ocean models driving an atmospheric model (Stephens et al. [1998]) predict an equatorial peak in atmospheric potential oxygen ($APO \approx O_2 + CO_2$) . The definition of APO sees to it that the distribution is governed by the air-sea fluxes of CO_2 and O_2 as terrestrial O_2 and CO_2 fluxes tend to oppose each other. APO is more sensitive towards the solubility pump, as air-sea CO_2 and O_2 fluxes affect it in the same direction, while the biological pumps of the respective gases oppose each other. Hence the modeled equatorial peaks will be correlated to the solubility pump. Unfortunately there is no APO data available at the equator. But as the equatorial peak is the strongest signal in the respective models which, on the other hand, all fail to simulate the observed mean meridional APO gradient, it seems likely that modeled equatorial solubility pumps are deficient.

6. Summary

Abiotically induced air-sea oxygen fluxes were studied in an eddy-permitting numerical model of the North Atlantic.

The focus was on the quantitative validation of a relationship between air-sea heat fluxes and abiotically effected oxygen fluxes, a standard method used to distinguish between the solubility pump and the biological pump of oxygen in the ocean.

Model results indicate that this standard method yields annual cycles of air-sea oxygen flux biased high by 20 to 40% in the subtropical gyre, a result consistent with the admittedly sparse observations of argon supersaturation. The difference is ascribed to subsurface solar heating of water shielded from the atmosphere in spring / summer and subsequent mixed layer deepening in fall / winter which brings the (by then supersaturated) water back into contact with the atmosphere. While this leads to considerable overestimation of the seasonal O_2-flux cycle, errors should average out on the annual mean.

Another caveat which does not average out on annual and longer time scales is that this method does not account for mixing processes producing oversaturation due to the nonlinear relationship between oxygen saturation and temperature. The model predicts oceanic outgassing at the equator enhanced by $\approx 0.25\, mol\, O_2/a/m^2$ and oceanic oxygen uptake decreased by $\approx 0.5\, mol\, O_2/a/m^2$ north of 40°N resulting from mixing. Biotically effected air-sea exchange in the North Atlantic corresponds to about $2\, mol/O_2/m^2/a$ (Oschlies and Kähler [2004] based on model results) so modeled oxygen fluxes induced by mixing amount to $\approx 25\%$ of the biotic estimate north of 40°N.

We presented evidence that in the model the equatorial estimate is massively influenced by numerical artefacts, but unfortunately we could not validate to assess the net mixing rates modeled as most of the supersaturation reaching the surface stemmed from regions featured by strong currents (Gulf Stream, Equatorial Undercurrent) where diapycnal mixing is not well constrained yet.

Quantifying oversaturation of the inert gas argon in the thermocline and boundary currents may help to constrain water mass conversion in the ocean interior which, in steady state, has to balance water mass formation at the sea surface.

Acknowledgments. We acknowledge funding by the Deutsche Forschungsgemeinschaft and very helpful discussions with Carsten Eden.

References

Bopp, L., C. L. Quéré, M. Heimann, A. Manning and P. Monfray, 2002: Climate-induced oceanic oxygen fluxes: Implications for the contemporary carbon budget. *Global Biogeochemical Cycles*, **16** (2), p. doi:10.1029/2001GB001445.

Dietze, H. and A. Oschlies, 2004 subm.: Modeling abiotic production of apparent oxygen utilisation in the oligotrophic subtropical North Atlantic. *Ocean Dynamics*.

Doney, S. C., 1996: A Synoptic Atmospheric Surface Forcing Data Set and Physical Upper Ocean Model for the U.S. JGOFS Bermuda Atlantic Time-Series Study (BATS) Site. *Journal of Geophysical Research*, **101**, p. 25,615–25,634.

Eden, C. and A. Oschlies, 2003 subm.: Effective diffusivities in models of the North Atlantic. Part I: subtropical thermocline. *Journal of Physical Oceanography*.

Ganachaud, A. and C. Wunsch, 2002: Oceanic nutrient and oxygen transports and bounds on export production during the World Ocean Circulation Experiment. *Global Biogeochemical Cycles*, **16** (4), p. doi:10.1029/2000GB001333.

Garcia, H. E. and L. I. Gordon, 1992: Oxygen solubility in seawater: better fitting equations. *Limnol. Oceanogr.*, **37(6)**, p. 1307–1312.

Gibson, J. K., P. Kallberg, S. Uppala, A. Hernandez, A. Nomura and E. Serrano, 1997: ECMWF Re-Analysis Project report series. *ERA description, Eur. Cent. for Medium-Range Weather Forecasting, Reading, UK*, **1**, p. 72pp.

Gruber, N., M. Gloor, S. Fan and J. Sarmiento, 2001: Air-sea flux of oxygen estimated from bulk data: Implications for the marine and atmospheric oxygen cycles. *Global Biogeochemical Cycles*, **15** (4), p. 783–803.

Haney, R. L., 1971: Surface thermal boundary conditions for ocean circulation models. *Journal of Physical Oceanography*, **1**, p. 241–248.

Jenkins, W. and S. Doney, 2003: The subtropical nutrient spiral. *Global Biogeochemical Cycles*, **17** (4), p. 1110, doi:10.1029/2003GB002085.

Jerlov, N. G., 1976: Marine Optics. *Elsevier New York*.

Keeling, R. F. and S. R. Shertz, 1992: Seasonal and interannual variations in atmospheric oxygen and implications for the global carbon cycle. *Nature*, **358**, p. 723–727.

Keeling, R. F., B. B. Stephens, R. G. Najjar, S. C. Doney, D. Archer and M. Heimann, 1998: Seasonal variations in the atmospheric O2/N2 ratio in relation to the kinetics of air-sea gas exchange. *Global Biogeochemical Cycles*, **12**, p. 141–163.

Ledwell, J. R., A. J. Watson and C. S. Law, 1998: Mixing of a tracer in the pycnocline. *Journal of Geophysical Research*, **103 (C10)**, p. 21,499–21,529.

Levitus, S., R. Burgett and T. P. Boyer, 1994: World Ocean Atlas 1994. Volume 3: Salinity. Noaa atlas nesdis 3, NOAA, Washington D.C.

Najjar, R. and R. Keeling, 2000: Mean annual cycle of the air-sea oxygen flux: A global view. *Global Biogeochemical Cycles*, **14** (2), p. 573–584.

Oschlies, A., 1999: An unrealistic high-salinity tongue simulated in the tropical Atlantic: another example illustrating the need for a more careful treatment of vertical discretizations in OGCMs. *Ocean Modeling*, **1**, p. 101–109.

Oschlies, A. and P. Kähler, 2004: Biotic contribution of CO_2 and O_2 and its relation to new production, export production, and net community production. *Global Biogeochemical Cycles*, **18**, p. doi:10.1029/2003/GB002094.

Oschlies, A., W. Koeve and V. Garçon, 2000: An eddy-permitting coupled physical-biological model of the North Atlantic. Part II: Ecosystem dynamics and comparison with satellite and JGOFS local studies data. *Global Biogeochemical Cycles*, **14**, p. 499–523.

Simonot, J. and H. L. Treut, 1986: A Climatological Field of Mean Optical Properties of the World Ocean. *Journal of Geophysical Research*, **91**, p. 6642–6646.

Smith, R., M. Maltrud, F. Bryan and M. Hecht, 2000: Numerical Simulation of the North Atlantic Ocean at 1/10°. *Journal of Physical Oceanography*, **30**, p. 1532–1561.

Spitzer, W. S. and W. J. Jenkins, 1989: Rates of vertical mixing, gas exchange and new production: Estimates from seasonal gas cycles in the upper ocean near Bermuda. *Journal of Marine Research*, **47**, p. 169–196.

Stephens, B., R. Keeling, M. Heimann, K. Six, R. Murnane and K. Caldeira, 1998: Testing global ocean carbon cycle models using measurements of atmospheric O_2 and CO_2 concentration. *Global Biogeochemical Cycles*, **12** (2), p. 213–230.

H. Dietze and A. Oschlies, Leibniz-Institut für Meereswissenschaften an der Universität Kiel, Düsternbrooker Weg 20, 24105 Kiel, Germany. (hdietze@ifm-geomar.uni-kiel.de; aoschlies@ifm-geomar.uni-kiel.de)

Danksagung

Diese Arbeit entstand in der *interdisziplinären Projektgruppe* des Leibniz-Instituts für Meereswissenschaften an der Universität Kiel.

Entscheidend für das Gelingen dieser Arbeit war die hervorragende Betreuung durch Andreas Oschlies. Vielen Dank Andreas, insbesondere für Deine Bereitschaft Dich in meine nicht immer so klar formulierten Probleme hineinzudenken sowie für steten, motivierenden Zuspruch.

Besonders möchte ich noch Carsten Eden und Paul Kähler hervorheben die mir viel beigebracht haben.

Vielen Dank auch an das Zentrallabor für Messtechnik, an die Rechenzentren, an die Mitarbeiter der Abteilung Theorie und Modellierung und an alle die in der "alten Botanik" hausen.

Der Deutschen Forschungsgemeinschaft verdanke ich die Finanzierung der letzten drei Jahre.

Außerdem bedanke ich mich bei allen, die für mich da sind und wissen, dass sie an dieser Stelle gemeint sind.